Adsorption of methylene blue and phenol on activated carbon prepared from Fox Nutshell by K_2CO_3 activator

Dissertation submitted to the

National Institute of Technology Rourkela

in partial fulfillment of the requirements

of the degree of

Master of Technology (Dual Degree)

in

Chemical Engineering

By

Bajun Hansdah

(Roll Number: 710CH1021)

under the supervision of

Prof. Hara Mohan Jena

May 2016

DEPARTMENT OF CHEMICAL ENGINEERING

NATIONAL INSTITUTE OF TECHNOLOGY

DEPARTMENT OF CHEMICAL ENGINEERING

NATIONAL INSTITUTE OF TECHNOLOGY

Supervisor's Certificate

This is to certify that the work presented in this dissertation entitled *"Adsorption of methylene blue and phenol on activated carbon prepared from Fox Nutshell by K_2CO_3 activator"* by *Bajun Hansdah*, Roll No-710CH1021, is a record of original research carried out by him under my supervision and guidance in partial fulfillment of the requirements of the degree of *M.Tech (Dual Degree)* in *Chemical Engineering*.

<Supervisor's Signature>
<Hara Mohan Jena>

ACKNOWLEDGEMENT

A project can never be completed without the help of a lot of people and the sound knowledge they provide in various aspects. The persons in the list that follow are the people who had some contribution for completing this project work.

First and foremost, I am deeply grateful for his valuable guidance, continuous support, insight, patience and encouragement of my supervisor, **Dr. Hara Mohan Jena**, without whose constant trust, gentle prodding, this project work would not have been completed.

I am indebted to the Department of Chemical Engineering for providing the necessary equipment and chemical supplies to fulfil this project. I also would like to thank the Head of the Department of Chemical Engineering, **Dr. P. Rath** for providing the platform to perform this project work.

I owe a depth of gratitude to all department faculties of Chemical Engineering Department, NIT, Rourkela for their small but valuableadvice related to project work. I would like to give special thanks to all staffs of the Chemical Engineering department for their all-time technical, moral support to carrying out the project.

I would also like to thank **Mr. Arvind Kumar, Ph.D. scholar** for his helpand for his valuable time to assist me in various ways.

Department of Metallurgical & Materials Engineering, Chemistry Department, and Ceramic Department supported a lot for carrying out different characterization tests and analysis, which were a crucial part for my project.

Finally, I thank to God and my loveable parents and family without them this would not bepossible. Their faith, support, and love for me are unbelievable, which gave me a predictable strength and patience in my life.

May 17, 2016

NIT Rourkela

Bajun Hansdah

ROLL NO: 710CH1021

Dedicated to
Parents and Family Members

LIST OF FIGURES

LIST OF TABLES

NOMENCLATURE

AC: activated carbon

q_e: Equilibrium adsorption capacity (mg g^{-1})

q_t: Adsorption capacity (mg g^{-1}) at different contact time t (min)

C_0: Initial concentration of adsorbate in solution (mg L^{-1})

C_t: Concentration of adsorbate in solution at time t (mg L^{-1})

C_e:Equilibrium concentration of adsorbate in solution (mg L^{-1})

V: Volume of solution (L)

V_m: volume of monolayer capacity (cm^3g^{-1})

q_{exp}: Experimental adsorption capacity (mg g^{-1})

N: Number of experimental data points

q_{cal}: calculated adsorption capacity predicted by the model (mg g^{-1})

k_1: Rate constant of the pseudo-first-order (min^{-1})

k_2: Rate constant of pseudo-second-order adsorption (g min^{-1} mg^{-1})

k_i: Intraparticle diffusion rate constant (mg g^{-1} $min^{-1/2}$)

q_m: Maximum adsorption capacity of the solid phase loading

R_L: Dimensionless separation factor

k_L: Langmuir constant (L mg^{-1})

k_F: Freundlich constant ((mg g^{-1})(L $mg^{-1})^{1/n}$)

1/n: Dimensionless heterogeneity factor

B: Heat of adsorption (L g^{-1})

A: Dimensionless Tempkin isotherm constant

Abstract

Water pollution occurs due to rapid urbanization and industrialization. Polluted water comes from different industries like petroleum, coal processing, textile, pharmaceutical, food processing, plastic, pesticide, paper and pulp etc. are highly toxic, and effect to the living being and our environment. There are many toxic compounds present in the polluted water like inorganic and organic compounds. Methylene blue and phenol are considered as matter of interest to remove because both are toxic in nature. Various treatment processes used for the removal of phenolic compounds and dyes are adsorption, microbial degradation, wet air oxidation, ion exchange etc. Low cost adsorbent such as activated carbons are best option for removal of methylene blue and phenol from aqueous effluents. Activated carbons were prepared from Fox nutshell as an agricultural waste by chemical activation method using K_2CO_3 activating agent. Preparation of activated carbons were carried out at different K_2CO_3/Fox nutshell ratios, carbonization temperatures and activation time, which had significant effect on the performances of activated carbons like BET surface area. Specific surface area of activated carbon was maximum as 1236 m^2/g at 800 ºC with activation duration of 1 h and at a K_2CO_3/Fox nutshell ratios mass ratio of 0.5. The porous properties, surface microstructure in addition to the surface functional groups of the prepared carbons were characterized by N_2 adsorption/desorption isotherm, SEM and FTIR, respectively. The results show that both the carbonisation temperature and impregnation ratio noticeably affected the BET surface area as well as micro and mesopore volumes. Batch studies of methylene blue dye and phenol adsorption were conducted to evaluate the effect of various experimental parameters like pH, temperature, adsorbent dose, and contact time effect. The equilibrium adsorption data of methylene blue and phenol on adsorbent were analysed by the Langmuir, Freundlich and Temkin isotherm models. The isotherm data are well described by the Freundlich isotherm model for methylene Blue and phenol adsorption. Inter-particle diffusion, Pseudo-first-order, pseudo-second order models were used to analyze the kinetic data obtained at different concentrations of both adsorbates. The adsorption kinetics was well described by the pseudo-second-order kinetic model for both MB and phenol solutions. For methylene blue and phenol maximum adsorption capacity are found to 499.17 mg/g and 29.52 mg/g, respectively at 30 ºC. Thermodynamic parameters such as the standard Gibbs free energy (ΔG), enthalpy (ΔH) and entropy (ΔS) obtained in this study indicated that the adsorption of methylene blue and phenol by prepared activated carbon is spontaneous, endothermic and entropy increase in the degree of freedom (or disorder).

Key words: Phenol, Methylene blue, Activated carbon (AC), Adsorption isotherm, Kinetics.

Chapter-1

Introduction and Literature Review

1. Introduction and Literature Review

1.1. Introduction

Due to the rapid urbanization and industrialization the municipality water and industrial effluent water are contaminated with the presence of organic compounds as well as inorganic compounds. Organic compounds originate from domestic sewage, urban run-off, industrial effluents and agriculture wastewater. These organic compounds are released as industrial effluent from palm oil refineries, pulp and paper mills, chemical spills, pharmaceuticals, and agricultural pesticides. Organic pollutants are present in the waste water as pesticides, fertilizers, hydrocarbons, phenols, plasticizers, biphenyls, detergents, oils, greases, pharmaceuticals, proteins and carbohydrates [Ali et al., 2012; Berrios, 2012; Nageeb, 2013; Crini, 2005]. Wastewater with organic pollutants contains large quantities of suspended solids which reduce the photosynthesis due to light availability to photosynthetic organisms and on settling out alter the characteristics of the river bed. During the decomposition process of these organic compounds the dissolved oxygen in the water may be consumed at a greater rate so that it can be replenished, also causing oxygen depletion and having several consequences for the water stream [Ali et al., 2012].

Toxic organic pollutants cause several problems to our environment, these are most common pollutants of great concern because of their toxicity, persistence, long-range transportability and bioaccumulation in animals [Burkhard and Lukasewycz, 2008; Ali et al., 2012], and travel long distances and persists in living organisms. Pollutants are carbon-based chemical compounds and mixtures that include industrial chemicals such as heavy metals, dyes, and phenolic compounds.

In Organic pollutants, the phenolic compound, is one of the major pollutants present in wastewater. The commercial production of a wide variety of resins occur by phenol as a source material. The phenolic resins, which are used as construction materials for automobiles and appliances, epoxy resins and adhesives, and polyamide for various applications. Phenolic compounds containing waste water comes from certain industries, like high-temperature coal conversion, petroleum refining, resin, and plastics, etc. Such aromatic hydroxyl compounds are considered as priority pollutants since they are harmful to organisms especially human as well as aquatic life, at low concentrations also it can be toxic when elevated present levels and are known or suspected to be carcinogens [Ozkaya, 2006]. Due to these unacceptable effects of the phenolic compound in water the World Health

Organization (WHO) has set an upper permissible limit of 1mg/l to regulate the phenol concentration in drinking water [WHO report, 2010]. To deal with the problem, we need to treat the wastewater and reuse it instead of leaving that as such.

Dyes consider as another type of organic pollutants. The textile, pulp, and paper industries are reported to utilize large quantities of a number of dyes; these pollutants may be found in wastewaters of many industries generating considerable amounts of coloured wastewaters, toxic and even carcinogenic, posing a serious hazard to aquatic living organisms [Roozbeh et al., 2013]. Dyes are one of the problematic groups; they are emitted into wastewater from various industries, mainly from the dye manufacturing and textile finishing and also from food colouring, cosmetics, papers and carpet industries. It is well known that the dye effluents from dyestuff manufacturing and textile industries may exhibit toxic effects on microbial populations. It can be toxic and carcinogenic to the mammalian animal. Most dyes used in textile industries are stable to light and are not bio-degradable. Furthermore, they are resistant to aerobic digestion [Ardejani et al., 2007].

Some efficient techniques for the removal of highly toxic organic compounds from water stream have drawn significant interest. Some methods such as coagulation, filtration with coagulation, precipitation, ozonation, ion exchange, reverse osmosis, adsorption, and advanced oxidation processes have been used for the removal of organic pollutants from the wastewater [Nageeb, 2013]. The various methods mentioned above have been found to be limited since they often involve high capital and operational costs [Nageeb, 2013]. On the other hand ion exchange and reverse osmosis are more attractive processes because the pollutant values can be recovered along with their removal from the effluents. Reverse osmosis, ion exchange, and advanced oxidation processes do not seem to be economically feasible because of their relatively high investment and operational cost [Kharud, 2012].

Among the possible techniques for water treatments, the adsorption process by solid adsorbents shows potential as one of the most efficient methods for the treatment and removal of organic contaminants in wastewater treatment. Adsorption has advantages over the other methods because of simple design and can involve low investment in term of both initial cost and land required. The adsorption processes are widely used for the treatment of industrial wastewater from organic and inorganic pollutants and meet the great attention from the researchers [Ahmaruzzaman, 2008; Berrios, 2012; Aghdas et al., 2014; Mohamed Nageeb]. In recent years, the search for low-cost adsorbents that have pollutant binding capacities has intensified [Ardejani et al., 2007; Rio, 2005]. Materials locally available such as natural materials, agricultural wastes, and industrial wastes can be utilized as low-cost

adsorbents. Activated carbon produced from these materials can be used as an adsorbent for water and wastewater treatment [Amokrane et al., 1997; Kumar and Jena, 2015].

Adsorption by activated carbons (ACs) is one of the most frequently used methods to remove phenolic and dye compounds from wastewater because ACs possesses perfect adsorption ability due to porous in nature. The heterogeneous surface of activated carbon is a consequence of both geometrical heterogeneity (porosity) as well as chemical heterogeneity. Geometrical heterogeneity is the result of differences in shape and size of pores, as well as vacancies, pits, etc. [Rio et al., 2005]. Chemical heterogeneity is connected with different functional groups at a surface, and with various surface contaminants. Functional groups and delocalized electrons of the graphitic structure determine the apparent chemical character of an activated carbon surface [Girodsa et al., 2009]. Some of the groups, e.g., carbonyl, carboxyl, phenolic hydroxyl and lactonic ones, are acidic.

1.2. Adsorption

Table 1.1 shows the advantage and disadvantage of different removal techniques. The term adsorption includes the uptake of gaseous or liquid components of the mixture from the external and internal surface of porous solid. In chemical engineering's study, adsorption is called the separation process during which specific components of one phase of liquid or gases are transferred onto the surface of a solid adsorbent [Amokrane et al., 1997]. Adsorption is well-known equilibrium separation process and an effective method for water decontamination application, adsorption has been found to be superior to other techniques for water reuse regarding initial cost, flexibility and simplicity of design, ease of operation and insensitivity to toxic pollutants [Gregorio and Harmel, 2006].

Table 1.1: Removal techniques of pollutants with their advantage and disadvantage [Kharud, 2012]

Removal techniques	Advantage	Disadvantage
Adsorption on Activated carbons	The most effective adsorbent, great, capacity, produce a high-quality treated effluent	Ineffective against dispersing and vat dyes, the regeneration, is expensive and results in loss of the adsorbent, non-destructive Process
Coagulation Flocculation	Simple, economically feasible	High sludge production, handling and disposal problem

Biodegradation	Economically attractive publicly acceptable treatment	Slow process, necessary to create an optimally favourable environment, Maintenance and nutrition requirements
Oxidation	Rapid and efficient process	High energy cost, chemicals required
Membrane Separations	Removes all dye types, produce a high-quality treated effluent	high pressure, expensive, incapable of treating a large volume
Ion-exchange	No loss of sorbent on regeneration, effective	Economic constraints, not effective for disperse dyes
Advanced oxidation process	No sludge production, little or no consumption of chemicals, efficiency for recalcitrant dyes	Economically unfeasible, formation of by-products, technical constraints
Selective	Economically attractive, regeneration is not necessary, high selectivity	Requires chemical modification, non-destructive process
Bio-adsorbents Biomass	Low operating cost, good efficiency and selectivity, no toxic effect on micro-organisms	Slow process, performance depends on some external factors (pH and salts)

1.2.1. Types of adsorption

The adsorption at surface or interface is large as a result of binding forces between atoms, molecules and ions of adsorbate and surface (Robert, 1989). According to the nature of forces involved, therefore, adsorption can conveniently be divided into two types:

(i) Physical adsorption (or physisorption) no exchange of electrons is observed between the adsorbent and the adsorbate. The adsorbate is held to the surface by physical and non-specific forces type Van der Waals and hydrogen binding, and multiple layers may be formed with approximately the same heat of adsorption. The heat of adsorption for physisorption is at most a few kcal mol^{-1}. Physical adsorption is a non-specific and a reversible process.

(ii) Chemical adsorption (or chemisorption) involves the reaction of transfer and sharing of electrons between the adsorb species and the adsorbent. The resulting chemisorption bond is usually stronger than the derived from the physical adsorption (tens of kcal mol^{-1}) and is consequently much stronger and more stable at high temperatures than physisorption. Only a single molecular layer can be adsorbed.

Table.1.2 For different biomass based activated carbons used for adsorption.

Activated carbon	Preparing method	Adsorbed adsorbate	adsorption(mg/g)/ % removal	Reference
Coconut (Cocos nucifera)	-	methylene blue	70.92	Hameed et.al., 2008
Rattan sawdust	Chemical activation	methylene blue	294.14	Hameed et.al., 2007
Rejected tea	Chemical activation	methylene blue	242.11	Nasuha and Hameed, 2011
Olive stone	Physical activation	methylene blue	0.858	Berrios et.al., 2012
Rattan sawdust	Chemical activation	phenol	149.25	Hameed and Rahman, 2008
Soybean straw	Chemical activation	phenol	278	Miao et.al., 2013
Wood particleboard	Physical activation	phenol	500	Girods et.al., 2009
Eucalyptus wood	Physical activation	phenol	80%	Tancredi et.al., 2004
Coconut shell	Physiochemical activation	phenol	205.8	Din et.al, 2009
Commercial activated carbon	Chemical activation	phenol	94%	Ozkaya, 2006
Coconut husk	Chemical activation	Cholorophenol	716.10	Hameed et.al., 2008

1.2.2. Adsorption Isotherm

When the retention of a solute on solid particles is investigated, the remaining solute concentration of the compound C (mol L^{-1} or kg L^{-1}) can be compared with the concentration of this compound retained on solid particles Q(mol kg^{-1} or kg kg^{-1}). The relationship Q = f(C) is named the ‘‘sorption isotherm’’. The uniqueness of this relation requires several conditions to be met: (i) the various reaction equilibria of retention/ release must have been reached, and (ii) all other physicochemical parameters are constant. The word ‘‘isotherm’’ was specifically chosen because of the influence of the temperature on sorption reactions; the temperature must be kept constant [Werth and Reinhard, 1997; Limousin et al., 2007]. The adsorption isotherm of dilute solutions are classified into four main classes, according to the nature of the slope of the initial portion of the curve (isotherm) and thereafter into sub-groups, based on the shapes of the upper part of curve: the main classes are S-curve, L-curve (Langmuir type), H-curve (high affinity) and C-curve (constant partition) (Fig.1.1).

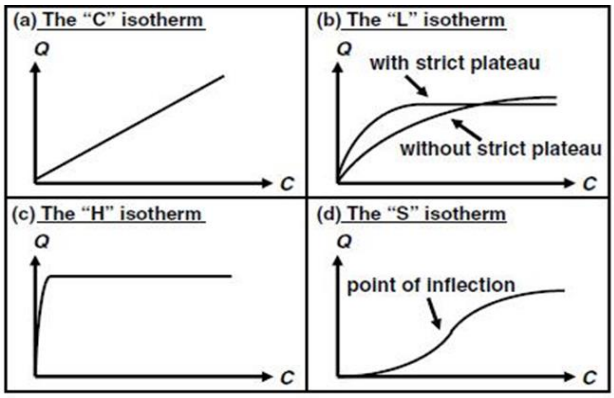

Fig. 1.1. Different types of the curve in isotherm study.

A) The ‘‘C’’ isotherm

The curve is a line of zero-origin (Fig. 1.1a). It means that the ratio between the concentration of the compound remaining in solution and adsorbed on the solid is the same at any concentration. This ratio is usually named ‘‘distribution coefficient’’ or ‘‘partition coefficient’’: K_d or K_p (L kg^{-1}). The ‘‘C’’ isotherm is often used as an easy-to-use approximation (for a narrow range of concentration or very low concentrations such as observed for trace pollutants) rather than an accurate description.

But the simplicity of this isotherm must not justify its use without verification; otherwise, it could lead to erroneous conclusions. For example, if the solid has a limited quantity of adsorption sites, the isotherm could be nonlinear because of a possible saturation plateau.

B) The ‘‘L’’ isotherm

The ratio between the concentration of the compound, remaining in solution and adsorbed on the solid, decreases when the solute concentration increases providing a concave curve (Fig. 1.1b). It suggests a progressive saturation of the solid. One usually makes two sub-groups: (i) the curve reaches a strict asymptotic plateau (the solid has a limited sorption capacity), and (ii) the curve does not reach any plateau (the solid does not show clearly a limited sorption capacity). But it often appears practically difficult to know if an isotherm belongs to the first or the second sub-group.

C) The ‘‘H’’ isotherm

This is only a particular case of the ‘‘L’’ isotherm, where the initial slope is very high (Fig. 1.1c). This case was distinguished from the others because the compound sometimes exhibits such a high affinity for the solid that the initial slope cannot be distinguished from infinity,

even if it does not make sense from a thermodynamic point of view by Toth, 1995 [Limousin et al., 2007].

D) The ‘‘S’’ isotherm

The curve is sigmoidal and thus has got a point of inflection (Fig. 1.1d). This type of isotherm is always the result of at least two opposite mechanisms. Non-polar organic compounds are a typical case: they have a low affinity with clays. But as soon as a clay surface is covered by these compounds, other organic molecules are adsorbed more easily. This phenomenon is called ‘‘cooperative adsorption’’ and is also observed for surfactants [Galan and Smith, 1975]. The presence of a soluble ligand can also provide a sigmoidal isotherm for metallic species. At low metal concentrations, the adsorption is limited by the presence of the ligand. The ligand must be saturated, and then the adsorption occurs normally. The point of inflection illustrates the concentration for which the adsorption overcomes the complexation.

1.2.3. Types of Adsorbents

Different types of adsorbents are classified into natural adsorbents and synthetic adsorbents. Natural adsorbents include charcoal, clays, clay minerals, zeolites, and ores. These natural materials, in many instances, are relatively cheap, abundant in supply and have significant potential for modification and ultimately enhancement of their adsorption capabilities. Synthetic adsorbents are prepared from agricultural products and wastes, household wastes, industrial wastes, sewage sludge and polymeric adsorbents. Each adsorbent has its characteristics such as porosity, pore structure, and nature of its adsorbing surfaces. Many waste materials used include fruit wastes, coconut shell, scrap tyres, bark and other tannin-rich materials, sawdust, rice husk, petroleum wastes, fertilizer wastes, fly ash, sugar industry wastes, blast furnace slag, chitosan, and seafood processing wastes, seaweed and algae, peat moss, clays, red mud, zeolites, sediment and soil, ore minerals, etc. Activated carbons use as an adsorbent for organic as well as inorganic pollutants. Activated carbons are common adsorbents used for the removal of undesirable odour, colour, taste, and other organic and inorganic impurities from domestic and industrial wastewater owing to their large surface area, microporous structure non-polar character and due to its economic viability. The major constituent of activated carbon is the carbon that accounts up to 95% of the mass weight. In addition, active carbons contain other hetero atoms such as hydrogen, nitrogen, sulfur, and oxygen. These are derived from the raw source material or become associated with the carbon during activation and other preparation procedures [Amokrane et al., 1997].

1.3. Activated Carbon

Carbon is the chemical element with symbol C and atomic number 6; it is nonmetallic and tetravalent making four electrons to form covalent chemical bonds. All the carbon materials composed of the carbon element has unique bonding with other elements and with itself. Depending on the type of hybridization of carbon atoms, the main allotropic forms of carbon are classified as graphite, diamond, and fullerene.

Activated carbon is an amorphous carbon-based material which has a highly developed porosity and an extended inter-particulate surface area and used for the removal of liquids and gaseous pollutants as well for the gas storage application [Bagheri and Abedi, 2009]. Activated carbons contain mainly micropores, but they also contain meso and macropores, which is very significant in helping contact of the adsorbate molecules to the interior of carbon particles (Ahmad et al. 2010). These pores can be classified into three categories (IUPAC Manual., 1972) i.e. Micropores <2 nm, Mesopores 2-50 nm, Macropores >50 nm. Adsorption by activated carbons (ACs) is one of the most commonly used because ACs possesses perfect adsorption ability for that class of compounds.

1.3.1. The textural properties of the activated carbon

During the carbonization of the raw material in the preparation of activated carbon, the free elementary carbon atoms self-assemble to form elementary graphite crystallites which comprise 3 to 4 parallel hexagonal carbon ring layers (Fig.1.2.a).

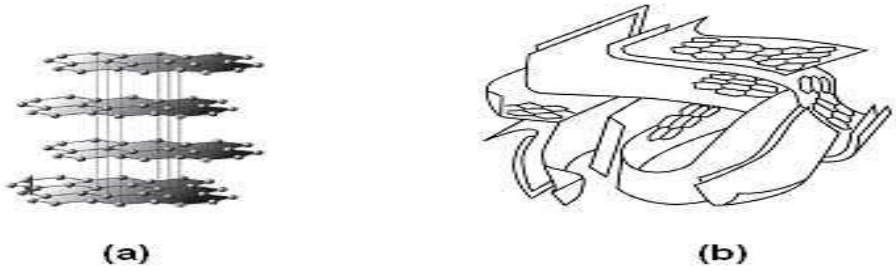

Fig.1.2. (a) Arrangement of carbon atoms in graphite crystal and (b) microstructure of the activated carbons

The major structure of AC is composed of microcrystalline (amorphous) graphitic-like sheets, called “basal planes,” which are randomly cross-linked and surrounded by some unpaired electrons. These particular architectural features make AC enormously porous and useful for applications in catalysis and adsorption with a wide range of molecules (Fig.1.2.(b)).

1.3.2. Surface functional groups

The adsorption capacity of the activated carbon is determined not only by the textural properties but also by the chemical nature of its surface [Bansal et al., 1988]. The surface of activated carbons is heterogeneous in nature; it consists of faces of graphite sheets and edges of such layers. The edge sites are much more reactive than the atoms in the interior of the graphite sheets; chemisorbed foreign heteroatom, mainly containing nitrogen, hydrogen, halogen and particularly oxygen, are predominantly located on the edges. Oxygen in the surface oxides is bound in the form of various functional groups. The surface chemical functional groups mainly derive from activation process, precursor, heat treatment, and post chemical treatment. The surface functional groups can be classified into two major groups; acidic groups consisting mainly carboxylic, lactones and phenols, and basic groups such as pyrone, chromene, ethers and carbonyls [Yang, 2003] (Fig.1.3).

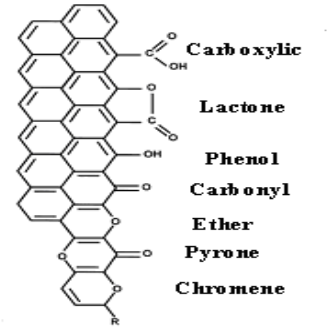

Fig.1.3. Surface functional groups of the activated carbon.

1.3.3. Classification of AC

The general classification of activated carbon is based on particle size, which are
(i) Powdered Activated Carbon (PAC)
(ii) Granular Activated Carbon (GAC) and
(iii) Activated Carbon Fiber (ACF)

1.3.3.1. Powdered AC

Powdered Activated Carbon (PAC), has a typical particle size of less than 0.1 mm and the common size of the particle ranges from 0.015 to 0.025 mm. Typical applications of PAC are industrial and municipal waste water treatments, sugar decolorization, in the food industry, pharmaceutical, and mercury and dioxin removal from a flue gas stream [Satyawali and Balakrishanan, 2009].

1.3.3.2. Granular AC

Granular Activated Carbon (GAC) has a mean particle size between 0.6 to 4 mm. It is usually used in continuous processes of both liquid and gas phase applications. GAC has an advantage over PAC, of offering a lower pressure drop along with the fact that it can be regenerated and therefore reused more than once. In addition to the proper micropore size distribution, its high apparent density, high hardness, and a low abrasion index made GAC more suitable over PAC for various applications [Scharf et al., 2010].

1.3.3.3. Activated Carbon Fibers (ACF)

ACFs are carbonized carbons which are subsequently heat treated in an oxidizing atmosphere. ACF began to be developed in 1970 using the precursor viscose rayon which mainly consists of cellulose. Later thermo-set polymer materials like saran and phenolic resins were used as precursors to produce ACF. A good ACF precursor must be non-graphitic and non-graphitizable carbon fibre which was isotropic in nature. From the end of the 1980s, interest is still centred on the production of ACFs from various inexpensive precursors.

1.3.4. Applications of ACs

AC is most useful in gas purification, decaffeination, and gold purification, metal extraction, water purification, sewage treatment, as medicine, as air filters in gas masks and respirators, as filters in compressed air and has many other applications (Table 1.3).

Table 1.3: Applications of AC in various fields and its uses

Applications	Uses
Medical uses	To treat poisonings and overdoses following oral ingestion
Environmental applications	Spill clean-up, Groundwater remediation, Drinking water filtration, Air purification, Volatile organic compounds capture from painting, dry cleaning, gasoline dispensing operations, and other processes.
Fuel storage	To store natural gas and hydrogen gas.
Gas purification	To remove oil vapors, odors, and other hydrocarbons from the air.
Chemical purification	To purify solutions containing unwanted colored impurities such as during a recrystallization procedure in organic chemistry
Distilled alcoholic beverage purification	AC filters can be used to filter vodka and whisky of organic impurities which can affect color, taste, and odor
Analytical chemistry applications	In 50% w/w combination with celite is used as stationary phase in low-pressure chromatographic separation of carbohydrates (mono, ditrisaccharides) using ethanol solution (5-50%) as mobile phase in analytical or preparative protocols

1.3.5. Preparation of Activated Carbons

There are two different processes for the preparation of AC: physical activation and chemical activation. Physical activation involves carbonization of carbonaceous material followed by the activation of the resulting char at high temperatures (800 – 1100 °C) in the presence of oxidizing agents such as CO_2 and steam. In chemical activation, the precursor is mixed with a chemical agent and then pyrolyzed at low temperatures (400 – 600 °C) in the absence of air. Chemical activation offers several advantages over physical activation as it is carried out in a Single step process, Lower activation temperature (<800 °C), Higher yields, Less activation time and therefore resulting in the development of a better porous structure [Khalili et al., 2000]. A typical preparation of AC involves carbonization of raw material in the absence of oxygen, and activation of carbonized product [Wang et al., 2007].

1.3.5.1. Physical Activation

It consists of two steps- **carbonization** and **activation**.

1.3.5.1.1. Carbonization

Carbonization is an inert thermal process to convert the carbonaceous precursor into solid char and leaving other liquids and gaseous as by-products [Chattopadhyaya et al., 2006]. This takes place in the absence of air and at temperatures of 600 to 800 ºC.

1.3.5.1.2. Activation

Table 1.4: Literature review on physical activation of biomass.

Sl. No.	Activating agent	Biomass	Reference
1	Steam	Corn shell	Omer and Cafer, 2013
2	CO_2	Cherry stone	Nowicki et.al, 2015
		Corn shell	Omer and Cafer, 2013
3	Air	Olive tree	Roozbeh et.al, 2013

Activation is a sequence process to enhance the char porosity and to clean out the tar clogging pores; thus increasing the total surface area of the produced activated carbon [Turmuzi et al., 2004]. The precursor and preparation methods (activation) determine not only its porosity but also the chemical nature of its surface, which consequently establishes it's adsorptive and catalytic characteristics [Khalil et al., 2000]. Activation can be done either

physically, chemically or by a combination of both, known as a physiochemical method. Physical activation is the gasification of the resulting char with an activating agent such as CO_2, steam or air at a high temperature (800-1000 ºC) [Rio et al., 2005]; the char develops a porous structure. The most widely used activating gas is steam because for a given temperature, the activated carbon produced with steam has larger adsorptive capacity and wider pore size distribution than that produced with CO_2.

1.3.5.2. Chemical Activation

Table 1.5: Literature review on chemical activation of biomass.

Sl. No.	Activating agents	Biomass	Reference
1	K_2CO_3	Cotton stalk	Deng et.al, 2010
		Nutshells	Foo and Hameed, 2012
		Pineapple peel	Hayashi et.al, 2002
		Almond shell	Hayashi et.al, 2002
		Coconut shell	Hayashi et.al, 2002
		Oil palm shell	Hayashi et.al, 2002
		Pistachio shell	Hayashi et.al, 2002
		Walnut shell	Hayashi et.al, 2002
		Euphorbia rigida	Kılıc et.al, 2012
		Palm shell	Adinata et.al, 2007
2	$ZnCl_2$	Grape stalk	Erdem et.al, 2014
		Safflower seed	Angın et.al,2013
		Euphorbia rigida	Kılıc et.al, 2012
3	KOH	Rice husk	wang et.al, 2014
		Corn cobs	Bagheri and Abedi, 2009
		Cassava and Tapioca Flour	Pari et.al, 2014
		Cotton stalk	Hui Deng et.al, 2010
		Rambutan peel	Njoku et.al, 2014
		Euphorbia rigida	Kılıc et.al, 2012
4	H_3PO_4	Cotton stalks	Nahil and Williams, 2012
		Almond shell	Yuso et.al, 2014
		Zizania caduciflora	Liu et.al, 2014
		Eucalyptus camaldulensis	Heidari et.al, 2014
		Euphorbia rigida	Kılıc et.al, 2012

The two steps (carbonization and activation) are carried out simultaneously in one step. Initially, the precursor is mixed with a chemical activating agent, which acts as dehydrating agent and oxidant. Chemical activation offers several advantages over physical activation which mainly include (i) lower activation temperature (<800 °C) compared to physical activation temperature (800 °C-1100 °C), (ii) single activation step, (iii) higher yields, (iv)

short activation time. The most commonly used chemical activating agents are H_3PO_4, $ZnCl_2$, KOH, and K_2CO_3.

1.3.5.2.1. Chemical Activation with K_2CO_3 activating agent

Activated carbons are prepared by chemical activation with K_2CO_3 from five kinds of nutshells: almond shell (AM), coconut shell (CN), oil palm shell (OP), pistachio shell (PT) and walnut shell (WN). When prepared at 800 °C, the activated carbons from all the nutshells had the maximum specific surface areas. According to the maximum values of specific surface areas, the activated carbons prepared were classified into two groups: Group-L and Group-S; the former group included activated carbons with high specific surface area and the latter included those with lower specific surface area, respectively. It was found that K_2CO_3 effectively worked as an activation reagent, but differently in the temperature ranges below 800 and above 900 ºC. Due to impregnation, cellulose and hemi-cellulose were modified by K_2CO_3 and accordingly the weight loss behaviours of the nutshells were changed in the temperature range below 800 °C. In the temperature range above 900 ºC, carbon in the chars was removed as CO gas by the reduction of K_2CO_3 to increase the specific surface area and the pore volume. It was deduced that the difference between the specific surface areas of Group-L and those of Group-S correspond to the difference between weight loss behaviours in the temperature range above 900 °C [Hayashi et al., 2002].

The activated carbon was prepared from cotton stalk with activating agent K_2CO_3 under microwave radiation was investigated. The effects of different activation conditions on the adsorption capacities of activated carbon were studied. The frequency test (F-test) was utilized in statistics to analyse the significant effects of the factors. The properties of activated carbons prepared under optimum conditions were investigated using the following measurement: N_2 adsorption isotherms at −196 ºC, SEM and FTIR. Finally, the sample was used in removal of methylene blue. The results showed that radiation time and radiation power were the greatest impact factor on adsorption capacities of the activated carbon prepared with K_2CO_3.In addition, chemical activation could develop both microporosity and mesoporosity. The equilibrium data of the adsorption was well fitted to the Langmuir isotherm for prepared activated carbons [Deng et al., 2010].

Wood sawdust was converted into a high-quality activated carbon via microwave-induced K_2CO_3 activation. The operational variables including chemical impregnation ratio, microwave power and irradiation time on the carbon yield and adsorption capability were identified. The surface physical characteristics of activated carbon were examined by pore

structural analysis, scanning electron microscopy and nitrogen adsorption isotherms. The adsorptive behavior of activated carbon was quantified using methylene blue as model dye compound. The best conditions resulted in activated carbon with a monolayer adsorption capacity of 423.17 mg/g and carbon yield of 80.75%. The BET surface area, Langmuir surface area and total pore volume were corresponded to 1496.05 m^2/g, 2245.53 m^2/g and 0.864 cm^3/g, respectively. The findings support the potential to prepare high surface area and mesoporous activated carbon from wood sawdust by microwave assisted chemical activation [Foo and Hameed, 2012].

Table 1.6: ACs prepared by K_2CO_3 with BET surface area

Prepared activated carbon	**Activating agent**	**BET surface area (m^2/g)**	**Reference**
Wood sawdust	K_2CO_3	1496.05	Foo and Hameed, 2012
Kraft lignin	K_2CO_3	1013	Li et.al, 2013
Cotton stalk	K_2CO_3	621.47	Deng et.al, 2010
Almond shell	K_2CO_3	1200	Hayashi et.al, 2002
Coconut shell	K_2CO_3	<1800	Hayashi et.al, 2002
Oil palm shell	K_2CO_3	1200	Hayashi et.al, 2002
Pistachio shell	K_2CO_3	1800	Hayashi et.al, 2002
Walnut shell	K_2CO_3	<1200	Hayashi et.al, 2002
Euphorbia rigida	K_2CO_3	2613	Kılıc et.al, 2012

Preparation of activated carbons from Euphorbia rigida by chemical activation with different impregnation ratios was studied. K_2CO_3 was used as chemical activation agents and four impregnation ratios (25–50–75–100%) by mass were applied on biomass. Activation is applied to impregnated biomass samples at 700 ºC under sweeping gas in a fixed bed reactor. For determination of chemical and physical properties of the obtained activated carbons; elemental analysis was applied to determine the elemental composition (C, H, N, O) and FTIR spectra was used to analyse the functional groups. BET equation was used to calculate the surface areas of activated carbons. For understanding the changes in the surface structure, activated carbons were conducted to Scanning Electron Microscopy (SEM). Maximum BET surface area (2613 m^2/g) was reached with 75% K_2CO_3 impregnated biomass sample. Experimental results showed that impregnation types and ratios have a significant effect on the pore structure of activated carbon and E. rigida seems to be an alternative precursor for commercial activated carbon production [Kılıc et al., 2012].

The catalysts K_2CO_3 was used to prepared Kraft lignin activated carbon by simply mixing K_2CO_3 with Kraft lignin and subsequently activating at 800 ºC for 2 h under N_2 flow. The

precursor and catalysts were characterized by thermal gravity analysis (TGA), Fourier transform infrared (FTIR) spectroscopy, X-ray diffraction (XRD), X-ray photoelectron spectroscopy (XPS), scanning electron microscopy (SEM) and Brunauer–Emmett–Teller (BET) surface area. The catalytic performance of prepared catalysts was evaluated by trans-esterification of rape seed oil with methanol. The effects of various parameters on biodiesel yield were investigated. The biodiesel yield of 99.6% was achieved by using the catalyst prepared by 0.6 of K_2CO_3/kraft lignin mass ratio and activation at 800 ºC, under the trans esterification condition of 65 ºC, 2 h, methanol to rapeseed oil molar ratio of 15:1 and 3.0 wt.% catalyst (relative to the weight of rapeseed oil). The solid catalyst can be reused for 4 times and biodiesel yield remained over 82.1% for the fourth time [Li et al., 2013].

1.4. Research objectives

The main objectives of the present research work are summarized below:

- Investigate the effect of preparation conditions for producing activated carbons from Fox nutshell and determine the primary factor(s) that affect the activated carbon properties.
- Perform characterizations of the prepared activated carbons to determine their physical and chemical properties.
- Study the equilibrium adsorption capacity of a basic dye (Methylene Blue) and Phenol onto the prepared carbons.

1.5. Organization of the Thesis

This thesis comprises of four chapters in the form of Introduction and Literature Review, Materials and Methods, Preparation and Characterization of activated carbons by chemical activation method, and Adsorption studies of Methylene blue and Phenol, and Conclusion and scope of the future work.

- Chapter 1 Introduction and Literature Review.
- Chapter 2 Deals with the experimental setup and experimental procedure.
- Chapter 3 Characterization of the prepared activated carbons and results of the adsorption of the adsorbates onto prepared adsorbents in batch scale.
- Chapter 4 Deals with the overall conclusion. Future recommendations based on the research outcome are suggested.

Chapter-2

Materials and methods

2. Materials and methods

2.1. Raw Materials

The Fox nutshell collected from a local Fox nut (Euryale ferox) processing unit from Madhubani district of Bihar state. The Fox nutshell soaked with 0.5 N NaOH solution and left for 12 h to remove all impurities like mud and ash present in the Fox nutshell during harvesting and processing. Then Fox nutshell is being properly washed with distilled water until the washed solution's pH achieved about 7. The cleaned material dried at 110 ºC for 24 h for further experiments. The dried Fox nutshell is being crushed and sieved to obtain a particle size of range 1.4–2.0 mm and analytical reagents grade Merck chemicals used for the study.

2.2. Characterization of Precursor

The composition of the raw material is an important factor that dictates the selection of precursor for the AC preparation. Various properties of the precursor were characterized by following standard procedures.

2.2.1. Thermogravimetric Analysis

The Thermogravimetric analysis (TGA) profile of the raw material gives an approximation about the weight loss with respect to temperature due to the release of surface bounded water and volatile matter. TGA of the raw precursor was carried out by a thermogravimetric analyzer (Shimadzu, Japan). About 10 mg of the sample was taken in a silica crucible and subjected to pyrolysis under N_2 flow (30 ml/min) to 1000 °C with a heating rate of 5 ºC/min.

2.2.2. Proximate analysis

ASTM D3173-75 did the proximate analysis. This analysis is used to determine the moisture content, volatile content, and ash content of the precursor selected.

2.2.3. Elemental analysis

The elemental analysis was done by using Elemental CHNS analyser (Elementar, Germany), and is used to determine the amount of carbon, hydrogen, nitrogen and sulphur content present in the precursor.

2.3. Preparation of activated carbon

After its first stage of cleaning Fox nutshell were impregnated with K_2CO_3 with an impregnation ratio (w/w) chemical/biomass ratio of 0.25, 0.5:1, 0.75:1 and 1:1 after soaking for 24 hrs. It was dried for 24 hrs at 110 °C. The carbonization of impregnated samples executed at 700, 800 and 900 °C for 1 h holding time at 5 °C / min in the presence of an inert atmosphere as a nitrogen gas in a Tubular furnace. The resulting material was again washed with 5% HCl. Then it was washed with warm and cold distilled water till it reached to neutral pH and dried for 24 hours. Then the samples were stored in an air tight container till further use.

2.3.1. Proximate analysis

The **moisture content** was found by the oven-drying test method. A sample of carbon is put into a dry, closed capsule (of known weight) and weighed accurately. The capsule is opened and placed with the lid in a preheated oven (110°C). The sample was dried to constant weight and then was removed from the oven and with the capsule closed, cooled to room temperature. The closed capsule was weighed again accurately. The percentage weight loss was taken as the moisture content of the sample.

The percentage of **volatile matter** of the AC samples was determined by the ASTM 5832 method. The sample was taken in a crucible with cover (of known weight), and the covered crucible was placed in muffle furnace regulated at 950°C for 7 min. Then the covered crucible was cooled to room temperature in a desiccator, and the weight was recorded. The percentage weight loss was regarded as the percentage of volatile matter.

To determine the **ash content** by ASTM D2866-94 method, the sample of AC was taken in the crucible (of known weight) and then placed in the muffle furnace at 550°C and ash formation was considered to be completed when constant weight was achieved. The crucible was cooled to room temperature in a desiccator and the percentage weight of the sample remained was considered as ash content.

Fixed carbon is a calculated value, and it is the resultant of summation of percentage moisture, ash, and volatile matter subtracted from 100 as given in equation (2.1).

Fixed carbon (%) = 100 – (moisture, % + ash, % + volatile matter, %).....(2.1)

2.3.2. Elemental analysis

The ultimate analysis or elemental analysis was carried out by using CHNS analyzer. The contents of carbon, hydrogen, nitrogen and sulphur of the Fox nutshell and activated carbons were measured using an Elemental Analyzer (Elementar, Germany) and the oxygen percentage

was estimated by difference. The percentage of oxygen was calculated by the difference as given in equation (2.2).

Oxygen (%) = 100 – (C, % + H, % + N, % + S, %) **(2.2)**

2.3.3. Yield% of prepared activated carbons

The yield of AC was calculated on a chemical-free basis and can be regarded as an indicator of the process efficiency for the chemical activation process. The yield of AC was calculated as the percentage weight of the resultant AC divided by the weight of waste tire char (raw char) as given in equation (2.3).

$$\text{Yield}\% = \frac{\text{weight of activated carbon after carbonisation}}{\text{weight of the raw material}} \times 100 \qquad (2.3)$$

2.3.4. Surface area of AC

Nitrogen (N_2) gas adsorption-desorption isotherms on prepared ACs at liquid nitrogen temperature (77K) were carried out using an automatic adsorption unit, Autosorb–1 (Quanta Chrome). The samples were degassed at 300° C for 3 h before analysis so as to remove any adsorbed moisture or other impurities bound to the surface of the sample. Surface area values were calculated from the experimental adsorption isotherm over a relative pressure range of 0.01 to 0.3 using the standard BET (Brunauer, Emmett, and Teller) method. The BET equation is given as,

$$\frac{p}{v(p^0 - p)} = \frac{1}{v_m C} + \frac{C - 1}{v_m C}\left(\frac{p}{p^0}\right) \qquad (2.4)$$

where, V is the volume adsorbed at STP (cm^3g^{-1}), v_m is the volume of monolayer capacity at STP (cm^3g^{-1}), and the term C, the BET constant, are related to the energy of adsorption in the first adsorbed layer and its value is an indication of the magnitude of the adsorbent-adsorbate interactions.

2.3.5. Fourier transform infrared (FTIR)

The surface functional groups of the ACs were estimated by Fourier Transform Infrared (FTIR) spectroscopy (Thermo Scientific Nicolet™ iS10) analysis. The samples were prepared in the form of KBr pellets with the sample to KBr ratio 1:100. The frequency range was selected between 4000 cm^{-1} to 400 cm^{-1}using KBr pellets with 32 scan per sample with a resolution of 4 cm^{-1}.

2.3.6. Field emission scanning electron microscopy (FESEM)

The surface topography of the prepared activated carbon was observed by Field emission scanning electron microscopy (Nova NanoSEM 450). SEM was carried out to show the pore structure of prepared activated carbons. The sample preparation included mounting of the activated carbon samples onto a silicon covered stage and a light sputtering of electrically conductive gold film for 13 s due to the conductivity of the activated carbon. The excitation voltage used was 10 kV, and observations were made with magnifications of 500–30000X.

2.4. Adsorption study

2.4.1. Isotherm study

2.4.1.1. The Langmuir model

The Langmuir adsorption is valid for monolayer adsorption. It is a very common model and is based on reaction hypothesis Langmuir (1918). The solid is assumed to have a limited adsorption capacity q_m. All the adsorption sites (1) are assumed to be identical, (2) each site retains one molecule of the given compound and (3) all sites are energetically independent of the adsorbed quantity. The Langmuir isotherms model is described by equation (2.5):

$$\frac{C_e}{q_e} = \frac{1}{k_L q_m} + \frac{C_e}{q_m}, \qquad (2.5)$$

where q_m and K_L represent the maximum adsorption capacity and the Langmuir constant respectively. The essential characteristics of a Langmuir isotherm can be expressed regarding dimensionless constant separation factor R_L defined as

$$R_L = \frac{1}{(1 + k_L C_o)}, \qquad (2.6)$$

where C_o is the initial concentration. R_L values less than unity confirms the favourable uptake of the adsorbent.

2.4.1.2. The Freundlich model

The model is based on adsorption on the heterogeneous surface and is a widely met isotherm (‘‘L’’ or ‘‘H’’ isotherms). The first model is empirical (Van Bemmelen, 1888; Freundlich, 1906) and model which is known to be satisfactory for low concentrations is expressed by the equation 2.7:

$$q_e = k_F + {C_e}^{1/n}, \qquad (2.7)$$

Where q_e is the equilibrium sorption concentration of solute per gram of adsorbent (mg-g^{-1}); C_e is the equilibrium aqueous concentration of the solute (mg $^{-1}$L); k_F and n are Freundlich constants which are related to the adsorption capacity and the intensity of adsorption. The value of n>1 represents a favorable condition. The linear form of Eq. (4.6) is

$$\ln q_e = \ln k_F + \frac{1}{n} \ln C_e \,, \qquad (2.8)$$

2.4.1.3. The Temkin model

The Temkin equation isotherm assume that the heat of adsorption of all the molecule in the layer decreased linearly with coverage due to sorbent-sorbate interaction and that adsorption is being characterized by uniformity in distribution of the binding energy, up to some extent maximum binding energy. The Temkin isotherm can be expressed as

$$q_e = B \ln(A) + B \ln C_e \,, \qquad (2.9)$$

where (B=RT/b) and A, the equilibrium binding constant (L/mg) which corresponds to the maximum binding energy and constant B which is related to the heat of adsorption. A plot of q_e versus ln (C_e) is useful for the determination of the isotherm constant A and B.

2.4.2. Kinetic study

The kinetic of sorption is significant from the point of view that it controls the efficiency of the process. The characterization of the adsorbent surface is a crucial factor that affects the parameters rate and that diffusional resistance also plays a vital role in the overall transport of the solute. The kinetics of sorption that defines the efficiency of sorption of methylene blue dye and phenol were determined by the inter-particle diffusion, pseudo first order or pseudo second order models.

2.4.2.1. Pseudo first order model

The first order rate expression is given by Lagergren:

$$\ln(q_e - q_t) = \ln q_e - k_1 t \,, \qquad (2.10)$$

where, q_e and q_t are the amounts of adsorbate adsorbed (mg/g) at time t (min) and at equilibrium time, respectively, and k_1 is the rate constant of the adsorption (Rengaraj et al., 2001; Inbaraj and Sulochana, 2005).

For controlling of kinetics four steps were present, (a) mass transfer of adsorbates from boundary film to surface mass transfer of solute from solution to the boundary film (b) mass transfer of adsorbates from boundary film to surface, (3) sorption and ion exchange of adsorbates ions onto site, (4) internal diffusion of adsorbates. This step is assumed to be very

rapid and non-limiting in this kinetic analysis: sorption is a rapid phenomenon. The first, as well as the second steps, are external mass transfer resistance steps, which depends on various parameters such as agitation and homogeneity of the solution. The fourth one was particle diffusion resistance step.

2.4.2.2. Pseudo-second order model

The pseudo second order model can be represented in the following form (Ahmaruzzaman et al., 2008),

$$\frac{dq_t}{dt} = K_2(q_e - q_t)^2 \qquad (2.11)$$

Where, K_2 being the pseudo second order rate constant (g/mg .min).

After integrating the equation (2.11)

for boundary conditions, $q_t = 0$ at $t = 0$ and $q_t = q_t$ at $t = t$, the following equation is obtained

$$\frac{1}{q_t} = \frac{1}{(K_2 q_e{}^2)} + \frac{1}{q_e}.t \qquad (2.12)$$

$$h = K_2 q_e{}^2 \qquad (2.13)$$

The initial adsorption rate h (mg/g.min), the pseudo second order constant K_2 the equilibrium sorption capacity (q_e), can be calculated from the slope and intercept of plot t/q_t vs. t.

2.4.2.3. Intraparticle diffusion model

The intra-particle diffusion model based on the theory proposed by Weber and Morris (1963) was used to identify the diffusion mechanism. According to this theory, the adsorbate uptake q_t varies almost proportionally with the square root of the contact time, $t^{1/2}$ rather than t.

$$q_e = K_i t^{\frac{1}{2}} + C \qquad (2.14)$$

where C is the intercept and k_i (mg g^{-1} $h^{-1/2}$) is the intra-particle diffusion rate constant. If intra-particle diffusion occurs, then q_e versus $t^{1/2}$ will be linear, and if the plot passes through the origin, then the rate limiting step is only due to interparticle diffusion. Otherwise, some other mechanisms along with intra-particle diffusion are involved. In most cases, this plot gives general features of three stages: initial curved portion, followed by an intermediate linear portion and a plateau. The initial sharper is due to the instantaneous adsorption or external surface adsorption (external mass transfer). The intermediate linear part is due to intra-particle diffusion, and the plateau arises from the equilibrium stage where interparticle diffusion starts to slow down because of the extremely low solute concentrations in the solution.

Chapter-3

Results and discussions

3. Results and discussions

3.1. Characterisation of ACs

3.1.1. Proximate and ultimate analysis

The results of the proximate and elemental analysis of the raw material and prepared activated carbon at impregnation ratio= 0.5 and 800 °C of activation temperature is tabulated in Table 3.1. From Table 3.1, the volatile matter of the prepared activated carbon is decreased by 18.5% than raw material of 70.1%. The ash content decrease while fixed carbon content of the activated carbon is increased. From Table 3.1, the carbon content of activated carbon is increased from 42.30 to 70.54 wt%. The hydrogen and oxygen content decreased from 4.30 to 1.5 wt%, and 52.51 to 27.31 wt% respectively.

Table 3.1: Proximate and ultimate analysis

Analysis	Raw material (wt%)	Activated carbon (wt%)
Proximate		
Moisture	4.0	5.6
Volatile matter	70.1	18.5
Ash	5.0	1.3
Fixed carbon*	20.9	74.6
Ultimate		
Carbon	42.30	70.54
Hydrogen	4.30	1.50
Nitrogen	0.82	0.62
Sulphur	0.07	0.0051
Oxygen*	52.51	27.31
* By difference		

3.1.2. Thermal characterization of Fox nutshell

Thermogravimetric analysis shows that the activation process can be divided into three stages. During the initial stage, the organic matter decomposes into the intermediate of smaller molar mass and releases the gaseous volatiles. The intermediates further decompose to form other

volatile species, tar, and char during the second stage. In the third stage, the solid residue regarded as activated carbon is obtained after the washing.

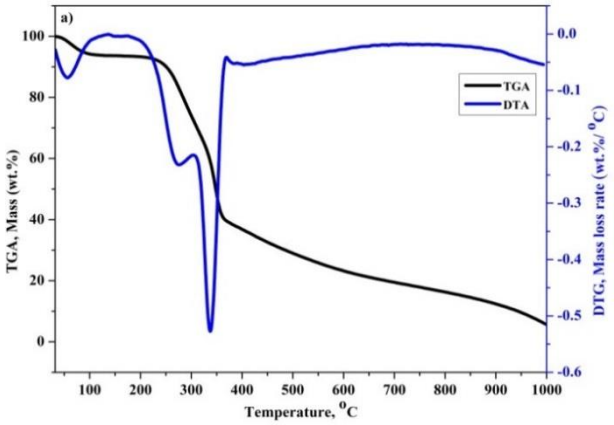

Fig. 3.1. TGA and DTA curves of Fox nutshell

The study of the thermal decomposition behavior of the Fox nutshell was performed by thermogravimetric analysis (TGA-DTA), and the result has been shown in Fig. 1.2. It can be seen that the thermal decomposition of Fox nutshell has taken place in three stages: 1) dehydration stage: room temperature to 230 °C; 2) acute weight loss stage: 260-365 °C; 3) slow weight loss stage: 375-800 °C. In the dehydration period of Fox nutshell, a little weight loss in TGA curve and the peaks at 65 °C in DTA curve is due to the loss of moisture. The major weight loss for Fox nutshell has been occurred at 260-365 °C due to the degradation of Fox nutshell and distillation of tar; finally, no major weight loss has been observed above 700 °C. The two peaks have been observed in the DTA curve for the Fox nutshell at 285 °C and 350 °C due to the thermal decomposition of hemicelluloses and cellulose, respectively. The mass loss is slower at high temperature due to the decomposition of lignin and also cracking reaction of C-C bonds also makes a contribution too small mass loss at the third stage of weight loss.

3.1.3. Yield % of the prepared Activated Carbons

The yield of product is the measure of the feasibility of preparing activated carbon from a given precursor. The effects of the activation temperature and impregnation ratio on the yields of activated carbon are shown in Fig. 3.2. The yields of activated carbons are decreasing with increasing activation temperature and impregnation ratio.

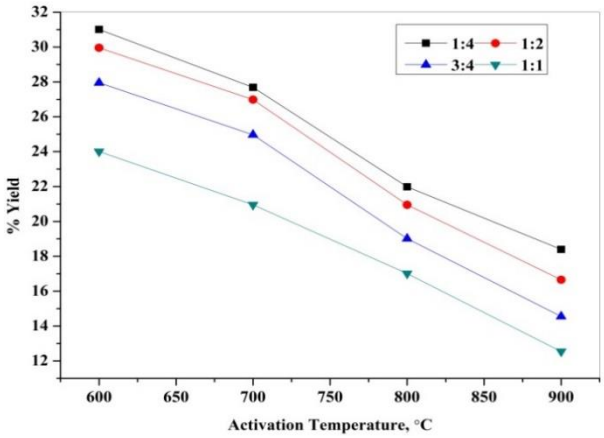

Fig. 3.2. The effects of carbonization temperature and impregnation ratio on the yield of activated carbon.

3.1.4. Textural characterization BET surface area analysis of AC

The textural characterization properties of prepared activated carbons were investigated by N_2 adsorption at 77K. The adsorption data were analyzed to calculate the BET surface area, total pore volume, micropore volume and mesopore volume. The adsorption-desorption isotherms and pore size distributions were also plotted using the BJH-method.

Table 3.2 shows BET surface area, total pore volume, micropore volume and mesopore volume of the activated carbons prepared at different carbonization temperatures and impregnation ratios. The surface area of the prepared activated carbons is found to be increased from 856 to 1236 m^2/g when the temperature was raised from 700 to 800 °C at an impregnation ratio of 0.5. The surface area decreases with increase in temperature above 800 °C. At 800, °C of activation temperature the BET surface area, total pore volume, micropore, and mesopore volume are 1236 m^2/g, 0.98, 0.68 and 0.3 cm^3/g, respectively. From Table 3.2, at the activation temperature of 800 °C, the impregnation ratio was varied, and it was found that the BET surface area, as well as the total pore volume and the micropore volume, increased with the increasing in the impregnation ratio up to 0.5. The trend was found to reverse for impregnation ratio more than 0.5.

Fig. 3.3 shows the nitrogen adsorption–desorption isotherms for the prepared activated carbon of maximum surface area at −196 ºC. According to the International Union of Pure and Applied Chemistry (IUPAC) classification, the isotherm belongs to the type I, which represents that micropores are developed in the prepared activated carbon. A small H4-type hysteresis loop (wide knee) indicates the presence of mesoporosity associated with capillary condensation during the adsorption–desorption process [Kumar & Jena, 2015]. From Table 3.2, the

microporosity of the prepared activated carbons was decreased (69.81 to 60.71%) with the increase of both activation temperatures as well as impregnation ratios, but the mesoporosity was increased.

Table 3.2: Pore structure characterization of prepared activated carbon.

Activated carbon						
K_2CO_3 impregnation ratio = 1:2 **Activation temperature (°C)**						
AT	S_{BET} (m^2/g)	V_T (cm^3/g)	V_μ (cm^3/g)	V_m (cm^3/g)	V_μ/V_T (%)	V_m/V_T (%)
700	856	0.53	0.37	0.16	69.81	30.19
800	1236	0.98	0.68	0.30	69.39	30.61
900	902	0.61	0.42	0.19	68.85	31.15
Activation temperature: 800 °C **Impregnation ratio**						
1:4	464	0.58	0.42	0.16	72.41	27.59
1:2	1236	0.98	0.68	0.30	69.39	30.61
3:4	1022	0.84	0.55	0.29	65.48	34.52
1:1	867	0.56	0.34	0.22	60.71	39.29
S_{BET}: BET surface area, V_T: total pore volume, V_μ: micropore volume, V_m: mesopore volume						

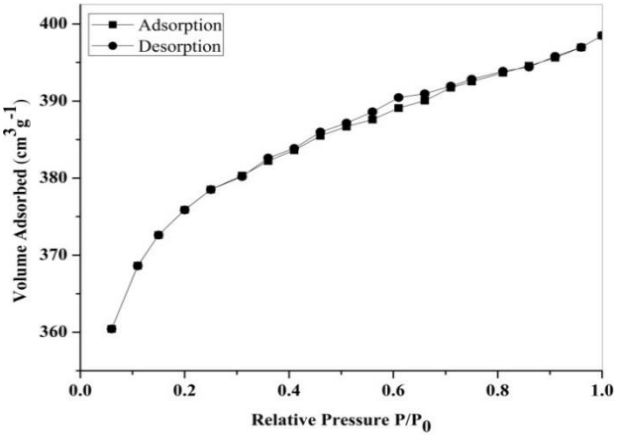

Fig. 3.3. N_2 adsorption–desorption isotherms of the prepared activated carbon at 800 ºC activation temperature and 0.5 impregnation ratio.

The pore size distribution of Fox nutshell activated carbon is shown in Fig. 3.4. The curve shows that the percentages of mesopore (with a pore size between 20 and 50 Å) are in a greater amount than those of micropore (with a pore size smaller than 20 Å) for the prepared activated carbon of maximum surface area. It demonstrates that Fox nutshell activated carbon has microporous and mesoporous in nature.

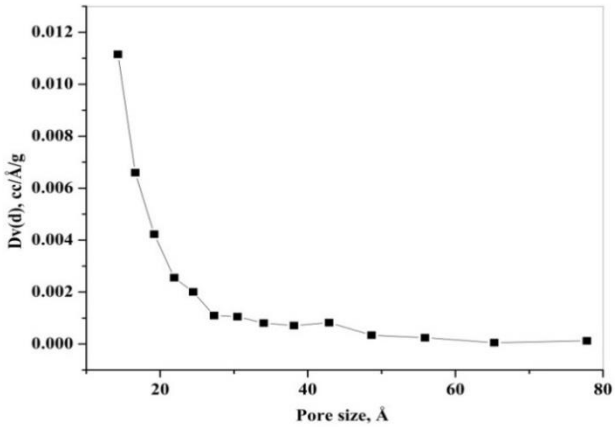

Fig. 3.4. Pore size distribution of the prepared activated carbon at 800 ºC activation temperature and 0.5 impregnation ratio.

3.1.5. FTIR of the activated carbon

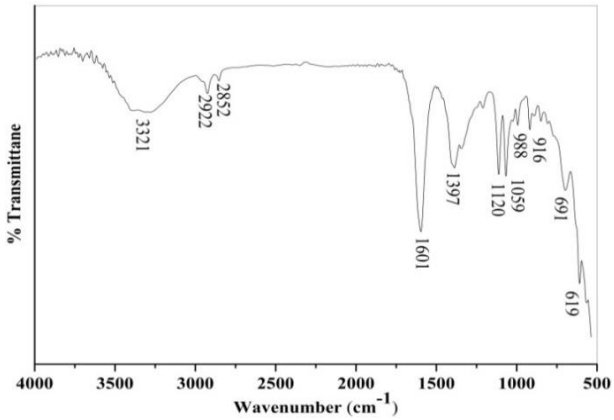

Fig. 3.5. FTIR spectra of activated carbon obtained at 800 °C activation temperature and 0.5 impregnation ratio.

The FTIR spectrum of the prepared activated carbon at 800 ºC activating temperature and 0.5 impregnation ratio is shown in Fig. 3.5. The peak at 3321 cm^{-1} corresponds to the presence of the hydrogen groups and adsorbed water. The bands at 2922 and 2852 cm^{-1} are indicated to aliphatic C-H stretching. The strong band at 1601 cm^{-1} is assigned to aromatic ring stretching vibrations (C=C). Broad bands at 1300–1000 cm^{-1} are assigned to C–O stretching in acids, alcohols, phenols, ethers, and esters. The bands at 691 and 619 cm^{-1} may be assigned to

aromatics substituted by aliphatic groups and O–H out-of-plane bending vibrations, respectively.

3.1.6. X - Ray Diffraction (XRD) analysis of the prepared activated carbon

XRD patterns of the developed activated carbon at 800 °C carbonization temperature and impregnation ratio of 1:2 is shown in Fig. 3.6. The XRD patterns have been exhibited broad peaks and absence of a sharp peak in activated carbon that reveals the predominantly amorphous structure of activated carbon; broad peak is an advantageous property for well-defined adsorbents. However, the occurrence of broad peaks at around 2θ = 26º and 43° is shown signs of formation of a carbonaceous crystalline structure, and that is resulting in better layer alignment.

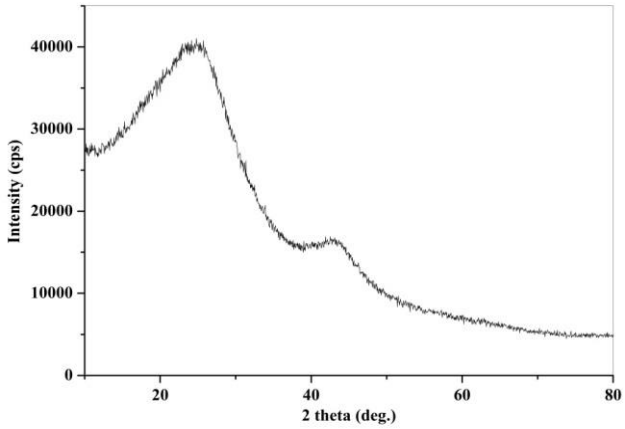

Fig. 3.6. XRD of activated carbon obtained at 800 °C activation temperature and 0.5 impregnation ratio.

3.1.7. FESEM analysis of Fox nutshell and prepared activated carbon

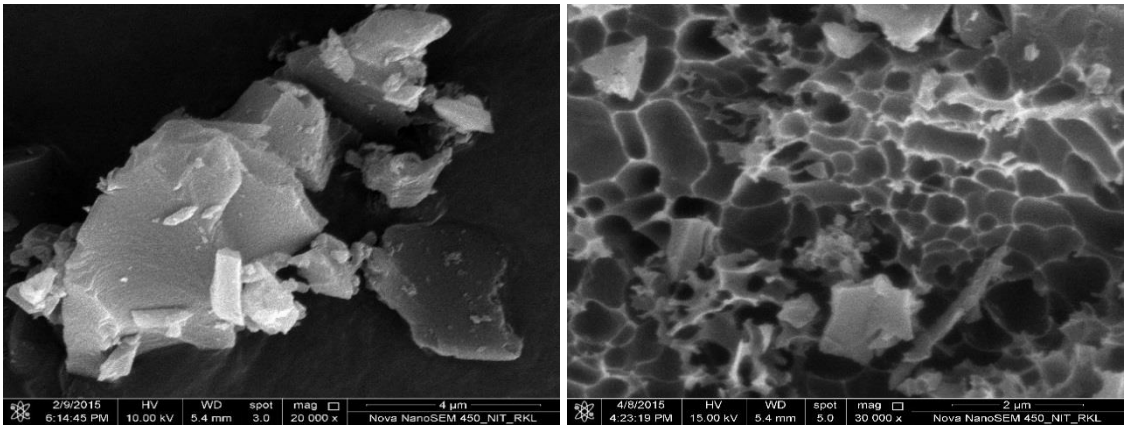

Fig. 3.7. FESEM analysis of Fox nutshell and AC.

The FESEM images of the Fox nutshell and developed activated carbon are shown in Fig. 3.7. There are significant differences between the surface morphology of the Fox nutshell and the prepared activated carbon with the maximum surface area. The surface of Fox nutshell has no pores on the surface, but more pores have been developed in the prepared activated carbon. The prepared activated carbon has large surface area due to highly porous than the Fox nutshell.

3.2. Adsorption study of methylene blue (MB) and phenol onto prepared activated carbon

3.2.1. Adsorption of methylene blue onto AC

3.2.1.1. Effect of process parameters

3.2.1.1.1. Effect of pH

The pH factor is very important in the adsorption process. The pH of a medium will control the magnitude of electrostatic charges which are impacted by the ionized methylene blue molecules. The effect of pH on removal methylene blue by prepared activated carbon was investigated over a pH range from 7-12. The experiments were performed at experimental conditions (initial MB concentration = 100.0 mg/L, adsorbent dose = 0.5 g/L, contact time = 3.0 h, and temperature = 30 °C). Figure 3.8 shows the higher removal of MB at basic pH.

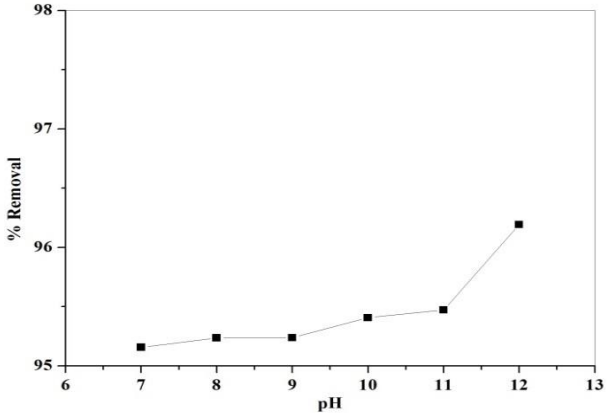

Fig. 3.8. Effect of pH on methylene blue % removal onto AC.

From figure-3.8, observed that the amount of dye adsorbed or % removal on AC is increased up to a maximum of 96.19% for derived AC. The basic dye (MB) gives positively charged ions when dissolved in water. In acidic medium, the positively charged surface of sorbent tends to oppose the adsorption of the cationic adsorbate. When pH of MB dye solution is increased the surface acquires a negative charge, thereby resulting in an increased adsorption of MB due to

an increase in the electrostatic attraction between positively charged dye and negatively charged adsorbent (Abd et al., 2009; Malik, 2003).

3.2.1.1.2. Effect of temperature

The effect of temperature on adsorption of methylene blue was studied at a concentration of 100 mg/l at different temperature (25, 30, 35 and 40). The experiments for the temperature effects were performed at experimental conditions (initial MB concentration = 100.0 mg/L, adsorbent dose = 0.5 g/L, contact time = 3.0 h, and pH = 12). Figure 3.9 shows the higher removal of MB at 30 ºC. From Fig. 3.9 the % removal of dye onto AC is a maximum of 93.19% at a temperature of 30 °C.

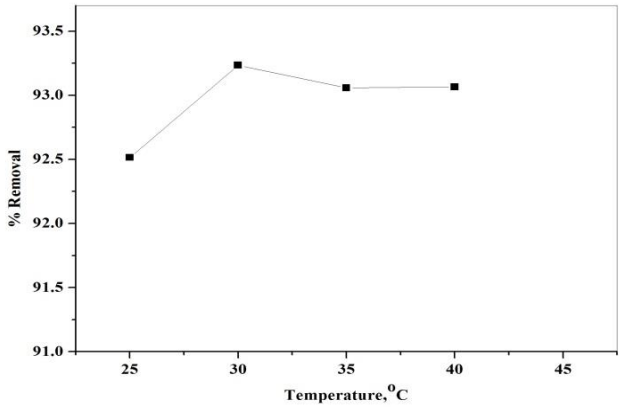

Fig. 3.9. Effect of temperature on methylene blue % removal of derived AC.

3.2.1.1.3. Effect of adsorbent dose

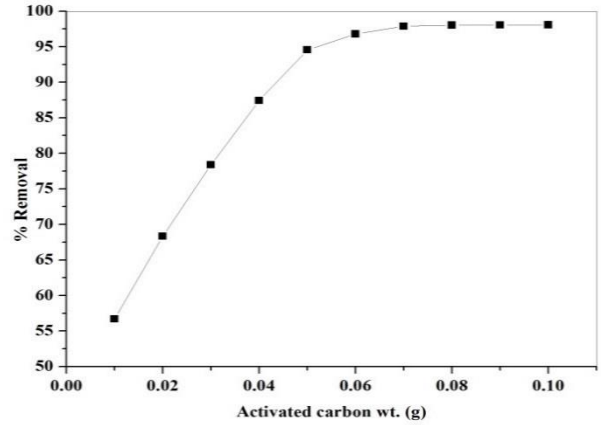

Fig. 3.10. Effect of AC dose on methylene blue % removal.

To study the effect of AC dose (g) on MB uptake, experiments were conducted at experimental conditions (initial MB concentration = 100.0 mg/L, contact time = 3.0 h, and pH = 12) while

the amount of adsorbent added was varied. Fig. 3.9 shows the effect of adsorbent dose on the % removal of MB. Activated carbon dosage was varied from 0.01 to 0.1 g/100 ml. The MB % removal increased with the increase in adsorbent dose up to 0.07 g significantly, and then increased slowly with further increase in adsorbent dose up to 0.08 g and after that remained unchanged. Thus, to get the better MB removal and to not consume a significant quantity of adsorbent, 0.08 g was chosen as an optimal mass of the adsorbent for the further experiments. At equilibrium time, the % removal increased from 55.82 to 99.71%. The rise in colour removal was due to the rise in the available sorption surface sites on the prepared activated carbon.

3.2.1.1.4. Effect of contact time and initial MB concentration

Fig. 3.11 shows the effects of contact time on the adsorption of MB onto AC at different initial concentrations (100, 200, 300, 400 and 500 mg/L) at pH = 12 and temperature = 30 °C. Adsorption studies were carried out for 3 h. It can be easily observed that the adsorption capacity of MB on AC drastically increased during the initial stage and then at a slow speed. The growing trend stopped when a state of equilibrium was reached. AC adsorbent removed a larger amount of MB in the first 10 min of contact time, and the equilibrium was established in 60 min for all different absorbent concentration studied (see Fig 3.11).

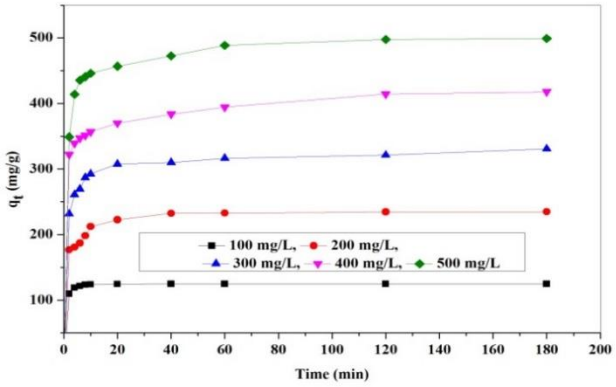

Fig. 3.11. Effect of different MB concentration with contact time.

A large number of vacant sites with active functional groups were available on prepared AC at an early stage of adsorption for the MB molecules. At a later stage, adsorption retarded due to the intra-specific competition among the MB molecules with the surface functional groups. The equilibrium adsorption increased from 249.88 mg/g to 968.74 mg/g when MB initial concentration enhanced from 100 mg/L to 500 mg/L. The higher mass transfer is because of increase in the driving force, i.e., the initial concentration of MB. From Fig. 3.12 the reverse behavior is observed in the case of % removal of MB, as the initial concentration increased from 100 mg/L to 500 mg/L then removal % of MB is decreased from 99.95% to 77.49%. The

decreased adsorption rates toward the end of experiments, indicates the possible monolayer formation of MB on the adsorbent surface (Abd et al., 2009; Nemer et al., 2010). Due to the lack of available active sites required for further uptake after attaining the equilibrium (Liang et al., 2010).

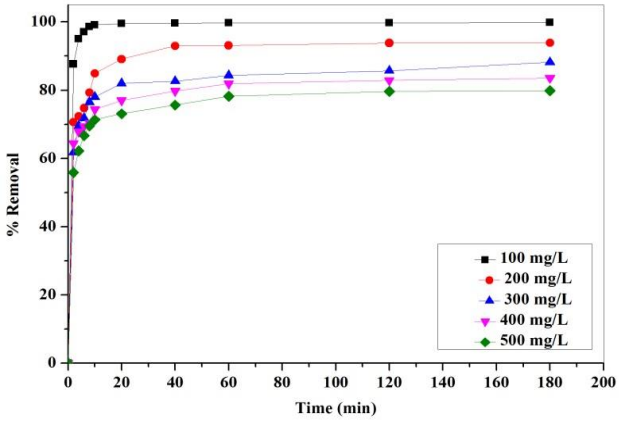

Fig. 3.12. % removal of MB onto AC with time at different concentration.

3.2.1.1.5. Adsorption isotherm study

At equilibrium state, the adsorption isotherm is very useful to describe how the adsorbed molecules distribute between the liquid phase and the solid phase. The Freundlich, Langmuir, and Temkin isotherm models were used for the adsorption isotherm. Fig. 3.13(a) shows a linear relationship of C_e/q_e versus C_e using experimental data obtained for MB adsorption Langmuir isotherm. The intercept and the slope of the plot result the q_m and k_L values and are tabulated in Table 3.3. The separation factor (R_L) is dimensionless quantity and it is an essential characteristic of the Langmuir isotherm [Hameed and Rahman, 2008] and is defined as:

$$R_L = \frac{1}{(1 + k_L C_o)}, \qquad (3.1)$$

where k_L is the Langmuir constant and C_o is the highest MB concentration (mg/L). The value of R_L indicates the type of the isotherm to be either unfavourable ($R_L > 1$), linear ($R_L = 1$), favourable ($0 < R_L < 1$) or irreversible ($R_L = 0$). The value of R_L was found to be 0.0007 for MB, and this again confirms that the Langmuir isotherm is favorable for MB adsorption on the AC under the conditions used in the present study.

A linear plot of ln q_e versus ln C_e confirms the validity of the Freundlich model and is shown in Fig. 3.13(b). The R^2 value estimates the goodness of the fit of the studied models. The data of Table 3.3 show that the Freundlich model (R^2=0.935) is the most adapted for fitting adsorption isotherms of MB on the prepared activated carbon than the Langmuir model (R^2=0.846).

From Table 3.3, the comparison of tested models for the description of equilibrium adsorption isotherms on the AC is as follows: Freundlich > Langmuir > Tempkin for MB.

Table 3.3: Isotherms constants of the models for MB adsorption

Langmuir			Freundlich			Tempkin		
q_m (mg/g)	k_L (L/mg)	R^2	k_F (mg/g(L/mg)$^{1/n}$)	n	R^2	b	A (L/g)	R^2
347.22	2.8615	0.846	164.7073	4.7094	0.935	47.0151	28.4793	0.780

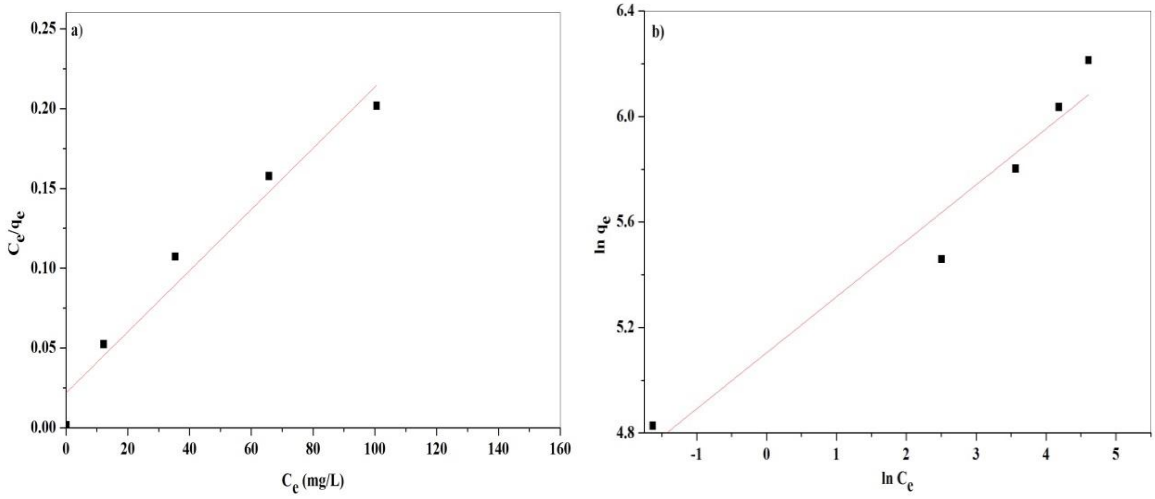

Fig. 3.13. (a) Langmuir and (b) Freundlich isotherm model for MB.

3.2.1.1.6. Adsorption kinetic study

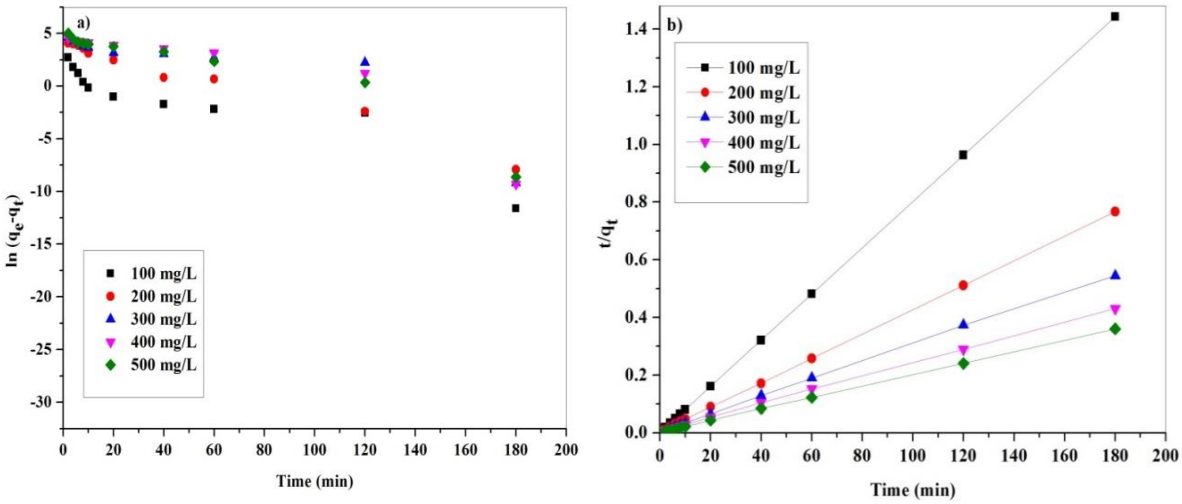

Fig. 3.14. (a) Pseudo-first order and (b) Pseudo-second order model of MB adsorption.

The derived kinetic parameters of pseudo-first order and pseudo second-order are listed in Table 4. The correlation coefficient of the second-order kinetic model (0.999) is greater than

for first-order kinetic model (< 0.999) (Table 4, Figs. 3.14(a) and (b)). This confirmed that the rate limiting step is chemisorption, involving valence forces through sharing or exchange of electrons (Bhattacharyya and Sharma, 2005).

Table 3.4: Pseudo-first order and Pseudo-second order for different initial MB concentrations.

Parameters	**MB** (mg/L)				
	100	200	300	400	500
$q_{e,exp}$ (mg g^{-1})	124.7541	234.67	330.70	417.75	499.17
Pseudo first-order					
$q_{e,cal}$ (mg g^{-1})	4.33	57.66	135.3	195.72	170.87
h_0 (mg g^{-1} min^{-1})	14.54	29	41.16	58.99	73.35
K_1(min^{-1})	0.1454	0.1448	0.137	0.147	0.147
R^2	0.836	0.9777	0.736	0.805	0.877
Δq (%)	32.17	18.96	16.69	17.72	21.92
Pseudo-second-order					
$q_{e,cal}$ (mg g^{-1})	124.84	236.41	330.03	420.17	502.51
K_2 (g (mg min)$^{-1}$)	0.0558	0.0037	0.0019	0.0012	0.0015
h_0 (mg g^{-1} min^{-1})	869.565	207.039	208.33	217.391	375.94
R^2	0.999	0.999	0.999	0.999	0.999
Δq (%)	0.024	0.24	0.067	0.19	0.22

3.2.1.1.7. Intraparticle study

Intraparticle diffusion model can identify the diffusion mechanisms and rate controlling steps in the adsorption process [Weber and Morris, 1962]. If the adsorption process follows the intra-particle diffusion model, then q_t versus $t^{1/2}$ will be linear, and if the plot passes through the origin, then intraparticle diffusion is the sole rate-limiting step. Otherwise, some other mechanism along with intra-particle diffusion is also involved. The parameters of the intraparticle diffusion model are given in Table 3.5. The intra-particle diffusion model (Fig. 3.15) presents multilinearity and does not pass through the origin, indicating that MB adsorption may take place in multiple steps, and the intra-particle diffusion is not the only rate limiting step.

Table 3.5: Intraparticle diffusion constants for the adsorption

C_0 (mg/L)	q_e(exp)	K_i (mgg^{-1} min$^{-1/2}$)	R^2	C
100	249.88	0.64	0.49044	243.19
200	483.84	10.91	0.39157	375.72
300	695.55	8.34	0.37184	612.13
400	836.07	9.34	0.38516	742.5
500	968.74	19.84	0.62039	763.88

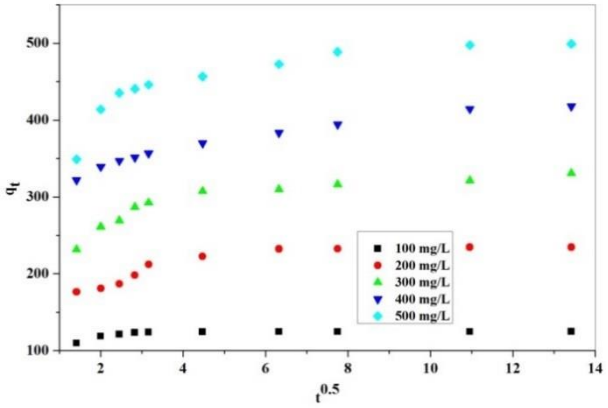

Fig. 3.15. Intraparticle diffusion for MB.

3.2.2. Adsorption of Phenol on AC

3.2.2.1. Effect of process parameters

3.2.2.1.1. pH effect

The adsorption of phenol was highly dependent on the initial pH of phenol solution that affected the surface charge of the AC and the degree of ionization of phenol. The effect of initial pH on the adsorption capacity of ACs for phenol is shown in Fig. 3.16. The effect of pH on removal phenol by prepared activated carbon was investigated over a pH range from 2-8. The experiments were performed at experimental conditions (initial phenol concentration = 100.0 mg/L, adsorbent dose = 0.5 g/L, contact time = 3.0 h, and temperature = 30 °C). Figure 3.18 shows the higher removal of phenol at pH=2. From Fig. 3.16 we observed that the amount of phenol adsorbed or % removal on AC is decreased. The pH effect can be explained by the difference in the surface chemistry of ACs and properties of phenol in solution. In acidic solution, the undissociated species of phenol were high, and the dispersion interactions predominated [Tzouet et al., 2008], which resulted in more phenol molecules adsorbed onto

the surface of AC. As the initial pH increased, phenol molecules started to dissociate into phenol anions, the adsorption amount of phenol decreased.

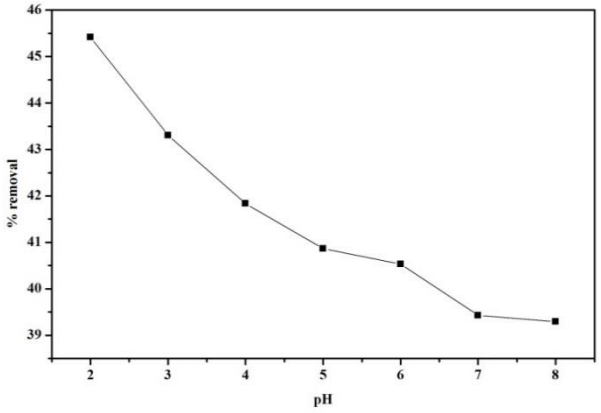

Fig. 3.16. Effect of pH on phenol % removal of derived AC.

3.2.2.1.2. Effect of temperature

The effect of temperature on adsorption of methylene blue was studied at a concentration of 100 mg/l at different temperature (25, 30, 35 and 40). The experiments for the temperature effects were performed at experimental conditions (initial phenol concentration = 100.0 mg/L, adsorbent dose = 0.5 g/L, contact time = 3.0 h, and pH = 2). Figure 3.17 shows the higher removal of 41.23% phenol at 35 ºC.

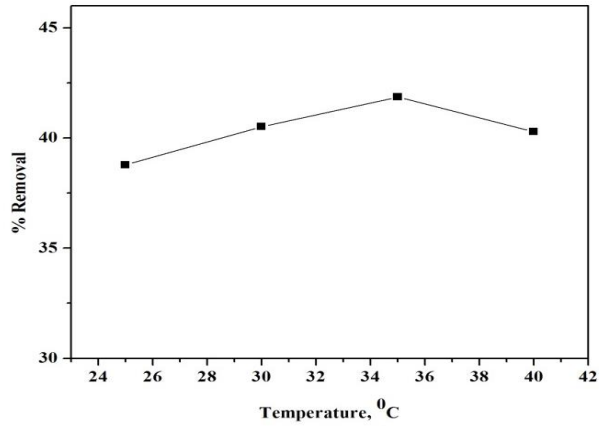

Fig. 3.17. Effect of temperature on phenol % removal of derived AC.

3.2.2.1.3. Effect of adsorbent dose

To study the effect of AC dose (g) on phenol uptake, experiments were conducted at experimental conditions (initial phenol concentration = 100.0 mg/L, contact time = 3.0 h, pH = 2, temperature = 35 ºC) while the amount of adsorbent added was varied. Fig. 3.18 shows the effect of adsorbent dose on the % removal of phenol. Activated carbon dosage was varied from 0.1 to 0.16 g/100 ml. The phenol % removal increased with the increase in adsorbent dose up to 1.2 g significantly, and then increased slowly with further increase in adsorbent dose up to 1.4 g and after that remained unchanged. Thus, to get the better phenol removal and to not consume a significant quantity of adsorbent, 1.4 g was chosen as an optimal mass of the adsorbent for the further experiments. At equilibrium time, the % removal increased from 79.82 to 99.71%. The rise in phenol removal was due to the rise in the available sorption surface sites on the prepared activated carbon.

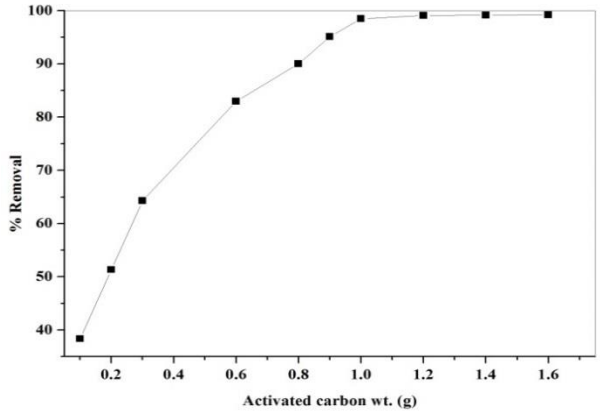

Fig. 3.18. Effect of dose on phenol % removal of AC.

3.2.2.1.4. Effect of initial phenol concentration and contact time

Fig. 3.19 shows the effects of contact time on the adsorption of phenol onto AC at different initial concentrations (100, 200, 300, 400 and 500 mg/L) at pH = 2 and temperature = 35 °C. Adsorption studies were carried out for 3 h. It can be easily observed that the adsorption capacity of phenol on AC drastically increased during the initial stage and then at a slow speed. The growing trend stopped when a state of equilibrium was reached. Prepared AC adsorbent removed a larger amount of phenol in the first 10 min of contact time, and the equilibrium was established in 60 min for all different phenol concentration studied (see Fig 3.19).

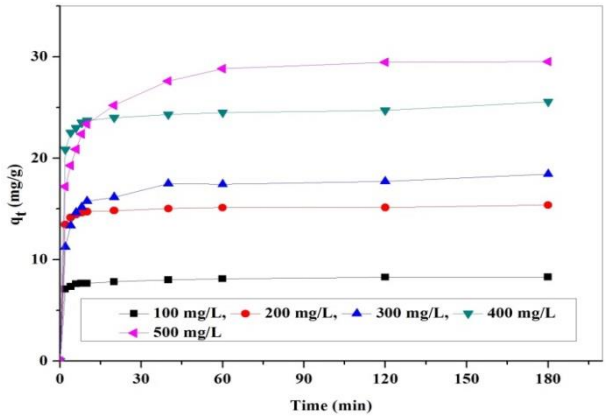

Fig. 3.19. Effect of different phenol concentration with different contact time.

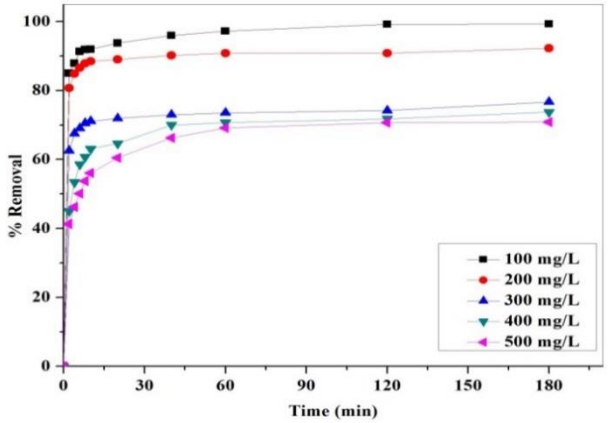

Fig. 3.20. % removal of phenol with contact time at different concentration.

A large number of vacant sites with active functional groups were available on AC at an early stage of adsorption for the phenol molecules. The adsorption of phenol occurs in ultramicro pores (d < 0.7 nm) and micropores (d < 2 nm), which are smaller in size than the molecular diameter of phenol (molecular diameter of phenol is 0.62 nm). An increment of the uptake was closely related to the greater mass driving force effect which permits more adsorbates to pass through from the bulk phase boundary to the carbon surface. A suggestion has been made that when the surface was almost filled up with adsorbates, the second mechanism of intra-particle diffusion will be activated, and this will enhance the adsorption further but in a very slow manner and very time consuming process as the reaction takes place inside the carbon matrix [Din et al., 2009]. The equilibrium adsorption increased from 249.88 mg/g to 968.74 mg/g when initial phenol concentration enhanced from 100 mg/L to 500 mg/L. The higher mass transfer is because of increase in the driving force, i.e., the initial concentration of phenol. From Fig. 3.20 the reverse behaviour is observed in the case of % removal of phenol, as the initial

concentration increased from 100 mg/L to 500 mg/L then removal % of MB is decreased from 99.95% to 77.49%.

3.2.2.1.5. Adsorption equilibrium study

Adsorption isotherm reflects the relationship between the amount of a solute adsorbed at constant temperature and its concentration in the equilibrium solution. It provides essential physicochemical data for assessing the applicability of the adsorption process as a complete unit operation. Langmuir and Freundlich isotherm models are widely used to investigate the adsorption process. The Langmuir isotherm was developed on the assumption that the adsorption process will only take place at specific homogenous sites within the adsorbent surface with a uniform distribution of energy level. Once the adsorbate is attached on the site, no further adsorption can take place at that site; which concluded that the adsorption process is monolayer in nature. Freundlich isotherm is based on the assumption that the adsorption occurs on heterogeneous sites with non-uniform distribution of energy level.

Figs. 3.21(a) and (b) exhibit the linear plots of Langmuir and Freundlich for phenol adsorption onto AC. The R^2 values show in Table 3.6 is evidence that the phenol adsorption in this study is well fitted to both Langmuir and Freundlich models; a possibility of mono and hetero layer phenol formation on the adsorbent surface. This observation is not rare as similar findings have been reported before [Hameed and Rahman, 2008].

The essential characteristics of the Langmuir isotherm can be expressed in terms of a dimensionless separation factor (R_L) [Hameed and Rahman, 2008] which is defined by

$$R_L = \frac{1}{(1 + k_L C_o)}, \qquad (3.2)$$

where k_L is the Langmuir constant and C_o is the highest phenol concentration (mg/L). The value of R_L indicates the type of the isotherm to be either unfavourable ($R_L > 1$), linear ($R_L = 1$), favourable ($0 < R_L < 1$) or irreversible ($R_L = 0$). The value of R_L was found to be 0.0000051 for phenol, and this again confirms that the Langmuir isotherm is favorable for phenol adsorption on the AC under the conditions used in the present study.

Temkin and Pyzhev considered the effects of indirect adsorbate/adsorbate interactions on adsorption isotherms. The heat of adsorption of all the molecules in the layer would decrease linearly with coverage due to adsorbate/adsorbate interactions. The linear form of Temkin isotherm is

$$q_e = B \ln(A) + B \ln C_e, \qquad (3.3)$$

where B=RT/b is related to the heat of adsorption (L/g), and A is the dimensionless Tempkin isotherm constant. This isotherm assumes that (i) the heat of adsorption of all the molecules in

the layer decreases linearly with coverage due to adsorbent–adsorbate interactions and that (ii) the adsorption is characterized by a uniform distribution of binding energies, up to some maximum binding energy [Hameed and Rahman, 2008]. The constant A and B together with the R^2 values are listed in Table 3.6. The correlation coefficient of Temkin isotherm equation (R^2 = 0.764) is lower than the Langmuir isotherm and Freundlich isotherm.

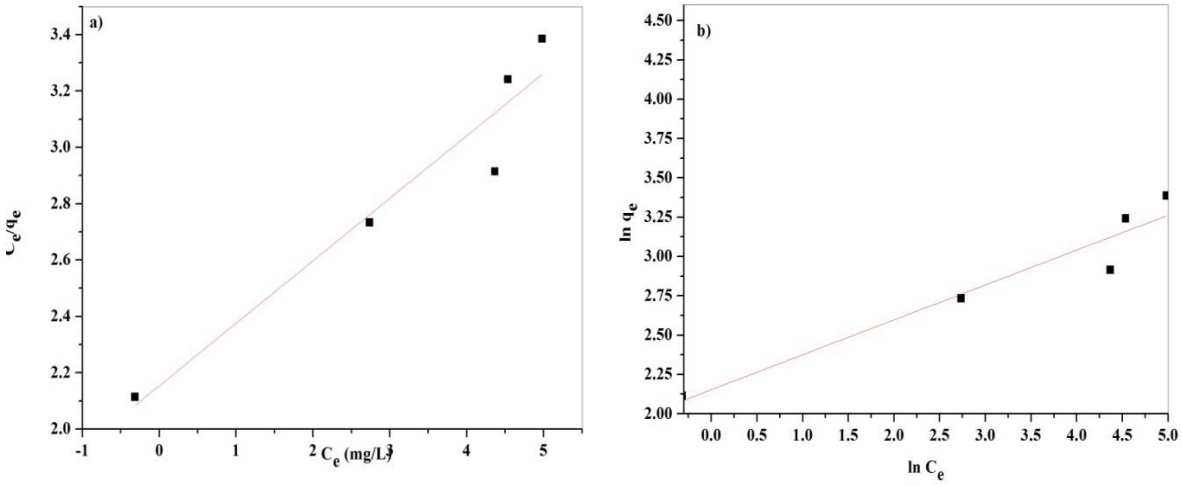

Fig. 3.21 (a) Langmuir and (b) Freundlich isotherm model for phenol.

Table 3.6: Isotherms constants for adsorption of phenol

C_0 (mg L^{-1})	Langmuir			Freundlich			Tempkin		
	q_m (mg/g)	k_F (mg/g(L/mg)$^{1/n}$)	R^2	k_F (mg/g(L/mg)$^{1/n}$)	k_L (L/mg)	R^2	b	A (L/g)	R^2
Phl	21.4546	8.614	0.861	8.614	391.865	0.9095	719.1507	9.832	0.764

3.2.2.1.6. Adsorption Kinetic study

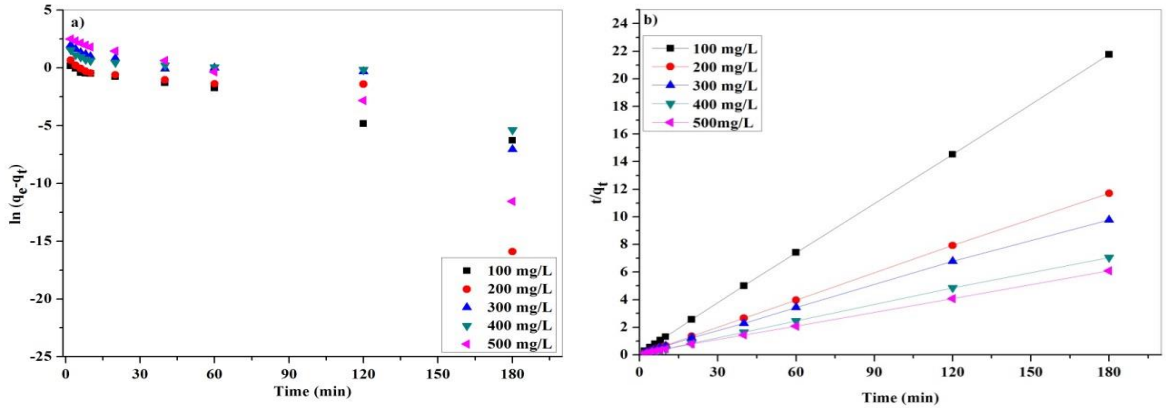

Fig. 3.22. (a) Pseudo-first order and (b) Pseudo-second order model for phenol.

Fig. 3.22 (a) should give a linear relationship with the slop K_1 and intercept of $\ln(q_e)$ from plot of $\ln(q_e-q_t)$ Vs. t (time). In many cases, the first-order equation of Lagergren does not fit well with the whole range of contact time and applies to the initial stage of the adsorption processes [Ho and McKay, 1999].

Table 3.7: Comparison of the pseudo-first-order and pseudo second-order for different initial phenol concentrations.

Parameters	**Phenol (mg/L)**				
	100	200	300	400	500
$q_{e,exp}$ (mg g^{-1})	8.27	15.38	18.43	25.55	29.52
Pseudo-first-order					
$q_{e,cal}$ (mg g^{-1})	1.005	3.05	6.2	3.78	18.74
h_0 (mg g^{-1} min^{-1})	8.3	32.2	27.3	26.8	79.5
K_1(min^{-1})	0.083	0.161	0.091	0.067	0.159
R^2	0.982	0.691	0.802	0.777	0.918
Δq (%)	29.28	26.72	22.12	28.40	12.17
Pseudo-second-order					
$q_{e,cal}$ (mg g^{-1})	8.30	15.35	18.41	25.41	29.98
K_2 (g $(mg\ min)^{-1}$)	0.143	0.117	0.026	0.037	0.033
h_0 (mg g^{-1} min^{-1})	9.853	27.55	8.97	24.009	29.976
R^2	0.999	0.999	0.999	0.999	0.999
Δq (%)	0.12	0.065	0.054	0.18	0.52

The slope and intercept of a plot of t/qt versus t (Fig. 3.22 (b)) were used to calculate the second-order rate constant K_2. It is more likely to predict the behaviour over the whole range of adsorption and is in agreement with the chemisorption mechanism being the rate controlling step [Dursun et al., 2005].

Table 3.7 lists the results of the constant rate studies for different initial phenol concentrations by the pseudo-first-order and second order models. For the pseudo-second-order model in Table 3.7, the rate constant decreased with the increase of the initial phenol concentration. The correlation coefficients obtained for the second-order kinetic model were greater than 0.999 at all the concentrations studied. Table 3.7 lists the Δq (%) values obtained. The results suggested

that the pseudo-second-order adsorption mechanism was predominant and that the overall rate of the phenol adsorption process appeared to be controlled by the chemisorption process [Ho and McKay, 1999]. The similar phenomena have also been observed in the adsorption of phenol on activated carbons prepared from beet pulp [Dursun et al., 2005] and plum kernels [Juang et al., 2000].

3.2.2.1.7. Intraparticle study

The intraparticle diffusion model to elucidate the diffusion mechanism, which is expressed as

$$q_t = k_i t^{0.5} + c\,, \qquad (3.4)$$

The constants were calculated and listed in Table 3.8. If the value of c is zero, then the rate of adsorption is controlled by intraparticle diffusion for the entire adsorption period. However, the plot of q_t against $t^{0.5}$ usually shows more than one linear portion, and if the slope of the first portion is not zero, then film (boundary layer) diffusion controls the adsorption rate at the beginning. As seen from Fig. 3.23, the plots were not linear over the whole time range, implying that more than one process affected the adsorption.

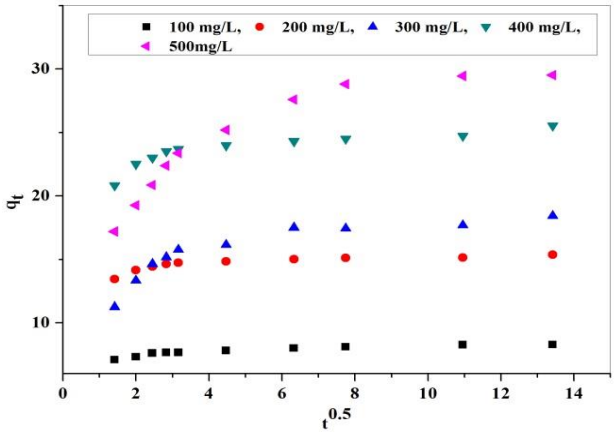

Fig.3.23. Intraparticle diffusion model for phenol.

Table 3.8: Intraparticle diffusion of the phenol adsorption

C_0 (mg/L)	q_e(exp)	K_i ($mgg^{-1}\,min^{-1/2}$)	R^2	C
100	19.84	0.17	0.766	17.98
200	38.25	1.48	0.667	22.85
300	55.25	1.52	0.7465	39.13
400	67.06	2.51	0.7545	40.37
500	75.37	2.41	0.7097	49.86

3.2.3. Thermodynamic studies

Thermodynamic parameters, such as a change in Gibbs free energy (ΔG), enthalpy (ΔH) and entropy (ΔS), were evaluated using Eqs. (3.5) (3.6) and (3.7):

$$K_C = \frac{q_{e(w/v)}}{C_e} \qquad (3.5)$$

$$\Delta G = -RT\ln K_C\,, \qquad (3.6)$$

$$\ln K_C = \frac{\Delta S}{R} - \frac{\Delta H}{RT}\,, \qquad (3.7)$$

where K_C is the equilibrium partition constant calculated as the ratio between sorption capacity (q_e) and equilibrium concentration (C_e), R is the gas constant (8.314 J/mol/K), and T is the temperature in Kelvin (K). From Eq. (3.7) a plot of ln K_C vs. 1/T (Figs. 10 and 11) gives ΔH and ΔS. The calculated thermodynamic parameters are given in Table 3.9. The negative value of ΔG indicates the spontaneous nature of MB and phenol adsorption onto the prepared activated carbon. Generally, a value of ΔG in between 0 and -20 kJ/mol is consistent with electrostatic interaction between adsorption sites and the adsorbing ion (physical adsorption) while a more negative ΔG value ranging from -80 to -400 kJ/mol indicates that the adsorption involves charge sharing or transferring from the adsorbent surface to the adsorbing ion to form a coordinate bond (chemisorption) (Sigh, 2000; AlOthman et al., 2014). As shown, the values of ΔG (-6.80 to -7.18 kJ/mol for MB and -0.27 to -0.58 kJ/mol for phenol) indicate a typical physical process.

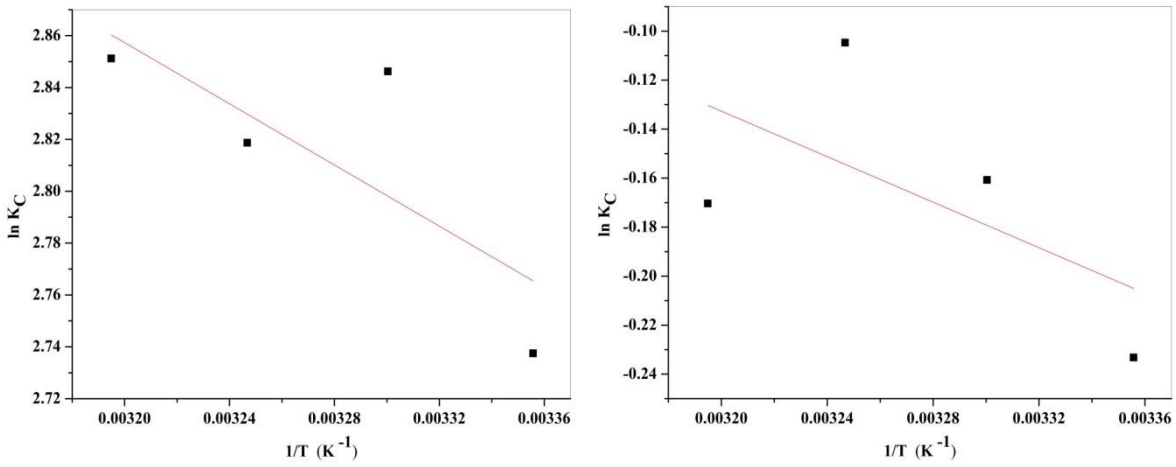

Fig. 3.24. Thermodynamic study of adsorption of (a) MB and (b) phenol onto prepared activated carbon.

As can be deduced from Figs. 3.24 (a) and (b), the positive value of ΔH suggests the endothermic nature of adsorption while the positive values of ΔS indicate an increase in the

degree of freedom (or disorder) of the adsorbed species. In general, the thermodynamic parameters indicate that the adsorption is spontaneous and endothermic for both MB and phenol.

Table 3.9: Thermodynamic parameters of adsorption of MB and phenol onto prepared activated carbon.

	T(K)	ΔG (kJ mol^{-1})	ΔH (kJ mol^{-1})	ΔS (J mol^{-1} K)
MB	298	-6.80	4.90	39.44
	303	-7.18		
	308	-7.21		
	313	-7.42		
Phenol	298	-0.58	3.86	11.26
	303	-0.40		
	308	-0.27		
	313	-0.44		

Conclusion

4. Conclusion

Removal of methylene blue dye and phenol from aqueous solutions by adsorption onto prepared activated carbon from Fox nutshell was studied. The prepared activated carbon was characterized by different analysis and test. High surface area activated carbon has been prepared from Fox nutshell by chemical activation with K_2CO_3. The experimental results confirm that the surface areas and pore volumes of the prepared activated carbons are strongly affected by the carbonization temperature and concentration of the activating reagent. The effect of impregnation ratio on surface area, total pore, and micropore volume of the activated carbon is stronger than the rise in the carbonization temperature. Activated carbon prepared by chemical activation of precursor by potassium carbonate with impregnation ratio (0.5) and 800 °C of activation temperature gives high surface area of 1236 m^2/g. FESEM image of prepared activated carbon confirms that well developed pores on the surface. The maximum % removal of MB and phenol are observed at pH 12 and 2, respectively. The equilibrium adsorption (q_e) is increased from 124.7541 to 499.17 mg/g when enhance MB initial concentration from 100 mg/L to 500 mg/L. The equilibrium adsorption (q_e) is increased from 8.27 to 29.52 mg/g with an increase in the initial phenol concentrations from 100 to 500 mg/L. The adsorption equilibrium isotherms on the AC is followed the following order: Freundlich > Langmuir > Tempkin for MB and phenol. Economic and environmental aspects point of view, the production of activated carbon with high surface area from Fox nutshell (a waste of the Fox nutshell industries). The prepared activated carbon at optimum conditions (800 °C carbonization temperature and 1:2 impregnation ratio) can be effectively used as adsorbents for various environmental applications such as removing hazardous compounds as MB and phenol from industrial waste gases and wastewater.

Future scope

1) Adsorption study of metallic compound on prepared activated carbon.

2) Activated carbon will prepare by using different precursor for adsorption study.

3) Optimization of process/operation variables using statistical method.

4) Adsorption studies will investigate through the continuous flow system method and fluidized bed system also be performed for best utilization of this adsorption process.

5) Methylene blue and Phenol desorption study will also be performed.

References

References

1. Adinata, D., Daud, W.M.A.W., Aroua, M.K., Preparation and characterization of activated carbon from palm shell by chemical activation with K_2CO_3. Bioresour. Technol. 98 (2007) 145-149.
2. Abd, E.L., Latif, M.M., Ibrahim, A.M., Adsorption, kinetic and equilibrium studies on removal of basic dye from aqueous solutions using hydrolyzed oak sawdust. Desalin. Water Treat. 6 (2009) 252–268.
3. Ahmaruzzaman., Adsorption of phenolic compounds on low-cost adsorbents: A review. Adv. Colloid Interface Sci. 143 (2008) 48–67.
4. Ali, I., Asim, M., Khan, T.A., Low cost adsorbents for the removal of organic pollutants from wastewater. J. Environ. Manage. 113 (2012) 170-183.
5. AlOthman, Z.A., Habila, M.A., Ali, R., Ghafar, A.A., Hassouna, M.S.E.D., Valorization of two waste streams into activated carbon and studying its adsorption kinetics, equilibrium isotherms and thermodynamics for methylene blue removal. Arab. J. Chem. 7 (2014) 1148–1158
6. Amokrane, A., Comel, C. and Veron., Landfill leachates pretreatment by coagulation-flocculation, PII: S0043-1354(1997)00147-4.
7. Angın, D., Altintig, E., Kose, T.E., Influence of process parameters on the surface and chemical properties of activated carbon obtained from biochar by chemical activation. Bioresour. Technol. 148 (2013) 542–549
8. Ardejani, F.D., Badii K., Yousefi, L.N., Mahmoodi, N.M., Arami, M., Shafaei, S.Z., Mirhabibi, A.R., Numerical modelling and laboratory studies on the removal of Direct Red 23 and Direct Red 80 dyes from textile effluents using orange peel, a low-cost adsorbent, Dyes Pigm. 73 (2007) 178-185.
9. Bagheri, N., Jalal, A., Preparation of high surface area activated carbon from corn by chemical activation using potassium hydroxide, Chem. Eng. Res. Des. 87 (2009) 1059–1064.
10. Bansal R.C., Donnet J.B., Stoeckli F., Active Carbon, Macel Dekker, New York, 1988.
11. Berrios, M., Martın, M.A., Martın, A., Treatment of pollutants in wastewater: Adsorption of methylene blue onto olive-based activated carbon. J. Ind. Eng. Chem. 18 (2012) 780–784.
12. Bhattacharyya, K.G., Sharma, A., Kinetics and thermodynamics of methylene blue sorption on neem (azadirachta indica) leaf powder. Dyes Pigm. 65 (2005) 51–59.
13. Burkhard, L.P., lukasewycz, M.T., Toxicity equivalency values for polychlorinated biphenyl mixtures, Environ. Toxicol. Chem. 27 (3) (2008) 529–534.
14. Chattopadhyaya, G., Macdonald, D.G., Bakhshi, N.N., Mohammadzadeh, J.S.S, Dalai, A.K., Adsorptive removal of sulfur dioxide by Saskatchewan lignite and its derivatives. Fuel 85 (2006) 1803–1810.

15. Crini, G., Peindy, H.N., Adsorption of C.I. Basic Blue 9 on cyclodextrin-based material containing carboxylic groups. Dyes Pigm. 70 (2006) 204-211
16. Crini, G., Recent developments in polysaccharide-based materials used as adsorbents in wastewater treatment. Prog. Polym. Sci. 30 (2005) 38–70.
17. Deng, H., Li, G., Yang, H., Tang, J., Tang, J., Preparation of activated carbons from cotton stalk by microwave assisted KOH and K_2CO_3 activation, Chem. Eng. J. 163 (2010) 373–381.
18. Din, A.T.M., Hameed, B.H., Ahmad, A.L., Batch adsorption of phenol onto physiochemical-activated coconut shell. J. Hazard. Mater. 161 (2009) 1522–1529.
19. Dursun, G., Cicek, H., Dursun, A.Y., Adsorption of phenol from aqueous solution by using carbonised beet pulp, J. Hazard. Mater. 125 (2005) 175–182.
20. Erdem, M., Ozdemir, I., Mehmet, S., Ramazan, O., Preparation and characterization of activated carbon from grape stalk by zinc chloride activation. Fuel Process. Technol. 125 (2014) 200–206.
21. Everett, D.H., Koopal, L.K., IUPAC 1972.
22. Foo, K.Y., Hameed, B.H., Mesoporous activated carbon from wood sawdust by K2CO3 activation using microwave heating, Bioresour. Technol. 111 (2012) 425–432.
23. Galan, M. A. and Smith, J. M., Adsorption of Sulfur Dioxide on Silica Gel-Rate and Equilibrium Parameters. J. Catal. 38 206-213 (1975).
24. Girods, P., Dufour, A., Fierro, V., Rogaume, Y., Rogaume, C., Zoulalian, A., Celzard, A., Activated carbons prepared from wood particleboard wastes: Characterisation and phenol adsorption capacities. J. Hazard. Mater. 166 (2009) 491–501.
25. Heidari, A., Younesi, H., Rashidi, A., Ali, A. G., Adsorptive removal of CO_2 on highly microporous activated carbons prepared from Eucalyptus camaldulensis wood: Effect of chemical activation, J Taiwan Inst Chem Eng 45 (2014) 579–588.
26. Yuso, A.M.D., Rubio, B., Izquierdo, M.T., Influence of activation atmosphere used in the chemical activation of almond shell on the characteristics and adsorption performance of activated carbons. Fuel Process. Technol. 119 (2014) 74–80.
27. Hameed, B.H., Rahman, A.A., Removal of phenol from aqueous solutions by adsorption onto activated carbon prepared from biomass material. J. Hazard. Mater. 160 (2008) 576–581.
28. Hameed, B.H., Mahmoud, D.K., Ahmad, A.L., Equilibrium modeling and kinetic studies on the adsorption of basic dye by a low-cost adsorbent: Coconut (Cocos nucifera) bunch waste. J. Hazard. Mater. 158 (2008) 65–72
29. Hameed, B.H., Ahmad, A.L., Latiff, K.N.A., Adsorption of basic dye (methylene blue) onto activated carbon prepared from rattan sawdust. Dyes Pigm. 75 (2007) 143-149.

30. Hayashia, J., Horikawa, T., Takeda, I., Muroyama, K., Ani, F.N., Preparing activated carbon from various nutshells by chemical activation with K_2CO_3, Carbon 40 (2002) 2381–2386.
31. Hesas, R.H., Niya, A.A., Daud, W.M.A.W., Sahu, J.N., Preparation of granular activated carbon from oil palm shell by microwave-induced chemical activation: Optimisation using surface response methodology, Chem. Eng. Res. Des. 91 (2013) 2447–2456.
32. Ho, Y.S., McKay, G., Pseudo-second order model for sorption processes, Process Biochem. 34 (1999) 451–465.
33. Inbaraj, B.S. and Sulochana, N., Use of jackfruit peel carbon (JPC) for adsorption of rhodamine-B, a basic dye from aqueous solution. Indian J. Chem. Technol. 13 (2006) 17-23.
34. Juang, R.S., Wu, F.C., Tseng, R.L., Mechanism of adsorption of dyes and phenols from water using activated carbons prepared from plum kernels, J. Colloid Interface Sci. 227 (2000) 437–444.
35. Khalili, N.R., Campbell, M., Sandi, G., Golas, J., Production of micro- and mesoporous activated carbon from paper mill sludge I. Effect of zinc chloride activation. Carbon 38 (2000) 1905-1915.
36. Kharub, M., use of various technologies, methods and adsorbents for the removal of dye. J. Environ. Res. Develop. 6 (2012).
37. Kılıc, M., Varol, E. A., Putun, A. E., Preparation and surface characterization of activated carbons from Euphorbia rigida by chemical activation with $ZnCl_2$, K_2CO_3, NaOH and H_3PO_4. Appl. Surf. Sci. 261 (2012) 247– 254.
38. Kumar, A., Jena, H. M., High surface area microporous activated carbons prepared from Fox nut (Euryale ferox) shell by zinc chloride activation. Appl. Surf. Sci. 356 (2015) 753–761.
39. Limousin, G., Gaudet, J.P., Charlet, L., Szenknect, S., Barthes, V., Krimissa, M., Sorption isotherms: A review on physical bases, modeling and measurement. Appl. Geochem. 22 (2007) 249–275.
40. Li, X.F., Zuo, Y., Zhang, Y., Fu, Y., Guo, Q.X., In situ preparation of K2CO3 supported Kraft lignin activated carbon as solid base catalyst for biodiesel production. Fuel 113 (2013) 435–442.
41. Liang, S., Guo, X., Feng, N., Tian, Q., Isotherms, kinetics and thermodynamic studies of adsorption of Cu2+ from aqueous solutions by Mg2+/K+ type orange peel adsorbent. J. Hazard. Mater. 174 (2010) 756–762.
42. Liu, H., Liang, S., Gao, J., Ngo, H. H., Guo, W., Guo, Z., Wang, J., Li, Y., Enhancement of Cr(VI) removal by modifying activated carbon developed from Zizania caduciflora with tartaric acid during phosphoric acid activation. Chem. Eng. J., 246 (2014) 168–174.
43. Malik, P.K., Use of activated carbons prepared from sawdust and rice-husk for sorption of acid dyes: a case study of acid yellow 36. Dyes Pigm. 56 (2003) 239–249.

44. Miao, Q., Tang, Y., Xu, J., Liu, X., Xiao, L., Chen, Q., Activated carbon prepared from soybean straw for phenol adsorption. J. Taiwan Inst. Chem. Eng. 44 (2013) 458–465.
45. Nahil, M.A., Williams, P.T., Pore characteristics of activated carbons from the phosphoric acid chemical activation of cotton stalks. Biomass Bioenergy 37 (2012) 142-149.
46. Nasuha, N., Hameed, B.H., Adsorption of methylene blue from aqueous solution onto NaOH-modified rejected tea. Chem. Eng. J. 166 (2011) 783–786.
47. Nemr, A.E., Abdel, W.O., Amany, E.S., Khaled, A., Removal of direct blue-86 from aqueous solution by new activated carbon developed from orange peel. J. Hazard. Mater. 161 (2009) 102–110.
48. Njoku, V.O., Foo, K.Y., Asif, M., Hameed, B.H., Preparation of activated carbons from rambutan (Nephelium lappaceum) peel by microwave-induced KOH activation for acid yellow 17 dye adsorption. Chem. Eng. J. 250 (2014) 198–204.
49. Omer, S., Cafer, S., Preparation and characterization of activated carbon from acorn shell by physical activation with H_2O–CO_2 in two-step pretreatment. Bioresour. Technol. 136 (2013) 163–168.
50. Ozkaya, B., Adsorption and desorption of phenol on activated carbon and a comparison of isotherm models, J. Hazard. Mater. 129(B)(2006) 158-163.
51. Pari, G., Darmawan, S., Prihandoko, B., Porous Carbon Spheres from Hydrothermal Carbonization and KOH Activation on Cassava and Tapioca Flour Raw Material. Procedia Environ. Sci. 20 (2014) 342 – 351.
52. Piotr, N., Justyna, K., Robert, P., Comparison of physicochemical and sorption properties of activated carbons prepared by physical and chemical activation of cherry stones. Powder Technol. 269 (2015) 312–319.
53. Rashed, M. N., Adsorption Technique for the Removal of Organic Pollutants from Water and Wastewater. Organic Pollutants - Monitoring, Risk and Treatment. Chapter 7.
54. Rengaraj, S., Moon, S.H., Kinetics of adsorption of Co(II) removal from water and wastewater by ion exchange resins. Water Res. 36 (2002) 1783–1793.
55. Rio, S., Brasquet, C.F., Coq, L.L., Courcoux, P., Cloirec, P.L., Experimental design methodology for the preparation of carbonaceous sorbents from sewage sludge by chemical activation—application to air and water treatments. Chemosphere 58 (2005) 423–437.
56. Satyawali, Y., Balakrishnan, M., Effect of PAC addition on sludge properties in an mbr treating high strength wastewater, Water Res. 43 (2009) 1577 – 1588.
57. Scharf, R.G., Johnston, R.W., Semmens, M.J., Hozalski, R.M., Comparison of batch sorption tests, pilot studies, and modeling for estimating GAC bed life. Water Res. 44 (3) (2010) 769-780.
58. Sigh, D., Studies of the adsorption thermodynamics of oxamyl on fly ash. Adsorpt. Sci. Technol. 18 (2000) 741–748.

59. Turmuzi, M., Daud, W.R.W., Tasirin, S.M., Takriff, M.S., Iyuke, S.E., Production of activated carbon from candlenut shell by CO2 activation. Carbon 42 (2004) 423–460.
60. Tancredi, N., Medero, N., Moller, F., Javier, P., Carina, P., Tomas. Phenol adsorption onto powdered and granular activated carbon, prepared from Eucalyptus wood Cordero. J. Colloid Interface Sci. 279 (2004) 357–363.
61. Tang, S., Lu, N., Li, J., Shang, K., Wu, Y., Improved phenol decomposition and simultaneous regeneration of granular activated carbon by the addition of a titanium dioxide catalyst under a dielectric barrier discharge plasma, Carbon 53 (2013) 380–390.
62. Tzou, Y.M., Wang, S.L., Liu, J.C., Huang, Y.Y., Chen, J.H., Removal of 2,4,6-trichlorophenol from a solution by humic acids repeatedly extracted from a peat soil, J. Hazard. Mater. 152 (2008) 812–819.
63. Wang, J., Technologies for water pollution control, Point Sources of Pollution: Local Effects and its Control – Vol. II.
64. Wang, J.P., Chen, Y.Z., Feng, H.M., Zhang, S.J., Yu, H.Q., Removal of 2,4-dicholophenol from aqueous solution by static-air-activated carbon fibers. J. Colloid Interface Sci. 313 (2007) 80–85.
65. Wang, L., Zhang, Z., Qu, Y., Guo, Y., Wang, Z., Wang, X., A novel route for preparation of high-performance porous carbons from hydrochars by KOH activation. Colloids Surf., A: Physicochemical Engineering Aspects 447 (2014) 183–187.
66. Weber, W.J., Morris, J.C., Advances in water pollution research: removal of biologically-resistant polluants from waste waters by adsorption. In: Proceedings of the International Conference on Water Pollution Symposium. Pergamon, Oxford, 2 (1962) 231–266.
67. Werth, C.J., Reinhard, M., Effects of Temperature on Trichloroethylene Desorption from Silica Gel and Natural Sediments. 1. Isotherms. Environ. Sci. Technol. 31 (1997) 689-696.
68. Werth, C.J., Reinhard, M., Effects of Temperature on Trichloroethylene Desorption from Silica Gel and Natural Sediments. 2. Kinetics. Environ. Sci. Technol. 31 (1997) 697-703.
69. WHO report, Persistent Organic Pollutants: Impact on Child Health, NLM Classification: WA 671 (2010).
70. Yang, T., Lua, A.C., Characteristics of activated carbons prepared from pistachio-nut shells by physical activation. J. Colloid Interface Sci. 267 (2003) 408–417.
71. Zheng, Z., Wang, Z., Nie, E., Li, J., Zhao, Y., Luo, X., Carbons prepared from Spartina alterniflora and its anaerobically digested residue by H3PO4 activation: Characterization and adsorption of cadmium from aqueous solutions. J. Hazard. Mater. 188 (2011) 29–36.